BMJ Open

# Cognitive and neuroimaging outcomes in individuals with benign and low-grade brain tumors receiving radiotherapy: a protocol for a prospective cohort study



| | |
|---|---|
| Journal: | *BMJ Open* |
| Manuscript ID | bmjopen-2022-066458 |
| Article Type: | Protocol |
| Date Submitted by the Author: | 11-Jul-2022 |
| Complete List of Authors: | Hardy, Sara; University of Rochester Medical Center, Department of Radiation Oncology; University of Rochester Medical Center, Department of Neurology<br>Finkelstein, Alan J.; University of Rochester, Department of Biomedical Engineering; University of Rochester Medical Center<br>Tivarus, Madalina; University of Rochester Medical Center; University of Rochester Medical Center, Department of Imaging Sciences<br>Culakova, Eva; University of Rochester Medical Center, Department of Surgery<br>Mohile, Nimish; University of Rochester Medical Center, Department of Neurology<br>Weber, Miriam; University of Rochester Medical Center, Department of Neurology; University of Rochester Medical Center, Department of Obstetrics and Gynecology<br>Lin, Edward; University of Rochester Medical Center, Department of Imaging Sciences<br>Zhong, Jianhui; University of Rochester, Department of Biomedical Engineering; University of Rochester Medical Center<br>Usuki, Kenneth; University of Rochester Medical Center, Department of Radiation Oncology<br>Schifitto, Giovanni; University of Rochester Medical Center, Department of Neurology, Department of Imaging Sciences<br>Milano, Michael; University of Rochester Medical Center, Department of Radiation Oncology<br>Janelsins-Benton, MC; University of Rochester Medical Center, Department of Radiation Oncology; University of Rochester Medical Center, Department of Surgery |
| Keywords: | RADIOTHERAPY, Neurological oncology < NEUROLOGY, Magnetic resonance imaging < RADIOLOGY & IMAGING, Radiation oncology < RADIOTHERAPY |
| | |

# Cognitive and neuroimaging outcomes in individuals with benign and low-grade brain tumors receiving radiotherapy: a protocol for a prospective cohort study

**Sara J Hardy[1,2,‡], Alan J. Finkelstein[3,4,‡], Madalina Tivarus[4,5], Eva Culakova[7], Nimish Mohile[2], Miriam Weber[2,6], Edward Lin[5], Jianhui Zhong[3,4,5,9], Kenneth Usuki[1], Giovanni Schifitto[2,5,8], Michael T Milano[1], Michelle C. Janelsins[1,7]**

**‡Authors contributed equally to the manuscript**

**Affiliations:**

[1]Department of Radiation Oncology, University of Rochester Medical Center, Rochester, NY, USA
[2]Department of Neurology, University of Rochester Medical Center, Rochester, NY, USA
[3]Department of Biomedical Engineering, University of Rochester, Rochester, NY, USA
[4]Center for Advanced Brain Imaging and Neurophysiology, University of Rochester Medical Center, Rochester, NY, USA
[5]Department of Imaging Sciences, University of Rochester Medical Center, Rochester, NY, USA
[6]Department of Obstetrics and Gynecology, University of Rochester Medical Center, Rochester, NY, USA
[7]Department of Surgery, University of Rochester Medical Center, Rochester, NY, USA
[8]Department of Electrical and Computer Engineering, University of Rochester, Rochester, NY, USA
[9]Department of Physics and Astronomy, University of Rochester, Rochester, NY, USA

**Corresponding author:**

**Sara J Hardy[1,2]**
sara_hardy@urmc.rochester.edu
[1]Department of Radiation Oncology, University of Rochester Medical Center, Rochester, NY, USA
[2]Department of Neurology, University of Rochester Medical Center, Rochester, NY, USA

**Keywords: neurological oncology, radiotherapy, magnetic resonance imaging, radiation oncology**

## ABSTRACT

**Introduction:** Radiation-induced cognitive decline (RICD) occurs in 50-90% of adult patients 6 months post-treatment. In patients with low grade and benign tumors with long expected survival, this is of paramount importance. Despite advances in radiation (RT) treatment delivery, better understanding of structures important for RICD is necessary to improve cognitive outcomes. We hypothesize that RT may affect network topology and microstructural integrity on MRI prior to any gross anatomical or apparent cognitive changes. In this longitudinal cohort study, we aim to determine the effects of RT on brain structural and functional integrity and cognition.

**Methods and Analysis:** This study will enroll patients with benign and low-grade brain tumors receiving partial brain radiotherapy. Patients will receive either hypofractionated (>2 Gy/fraction) or conventionally fractionated (1.8-2 Gy/fraction) RT. All subjects will be followed for 12 months, with MRIs conducted pre-RT and 6- and 12-months post-RT, along with a battery of neurocognitive tests and questionnaires. The study was initiated in late 2018 and will continue enrolling through 2024 with final follow ups completing in 2025. The neurocognitive battery assesses visual and verbal memory, attention, executive function, processing speed, and emotional cognition. MRI imaging protocols incorporate diffusion tensor imaging (DTI) and resting state fMRI (rs-fMRI) to assess structural connectivity (SC) and functional connectivity (FC), respectively. We will estimate the association between radiation dose, imaging metrics, and cognitive outcomes.

**Ethics and Dissemination:** This study has been approved by the Institutional Review Board (IRB). All results will be published in peer-reviewed journals and at scientific conferences.


## STRENGTHS AND LIMITATIONS OF THIS STUDY

- Evaluation of patients with benign and low-grade brain tumors helps to mitigate confounding factors such as variation in tumor biology and normal tissue infiltration and better parse out the effects of radiation.
- Prospective evaluation with baseline evaluation prior to radiation allows capture of subtle changes that would otherwise be missed since they would be within population norms
- Standard follow up period allows better understanding of trajectory of changes after radiation treatment for benign and low grade brain tumors.
- Multimodal imaging data in conjunction with neurocognitive battery provides a comprehensive evaluation of the biophysical effects of radiation in individuals with brain tumors.
- Use of open-source software assures transparency, reproducibility, and implementation of the proposed protocol by other investigators.
- Evaluation of RICD in the setting of hypofractionation, which has increasingly been utilized in benign and low grade brain tumors but evaluation of RICD in this population focuses on patients who receive conventionally fractionated radiation
- A significant limitation is heterogeneity of tumor type and laterality in patient population. However, excluding high grade tumors minimizes this limitation as much as possible while still allowing the study to be feasible at a single institution.

## INTRODUCTION

**Rationale and Evidence Gaps:** Cognitive impairment in patients with brain tumors has a major impact on quality of life and on the ability to function at work and in daily life (1-4). Deficits manifest clinically as impairments in multiple cognitive domains including memory, attention, and executive function (5, 6). The etiology is often multifactorial; contributing factors may include anxiety and/or depression, tumor location and pathology, comorbidities, and age, as well as effects from treatment (chemotherapy, surgery, and/or radiation therapy(7)). Notably, RICD is observed in more than 30% of patients at 4 months after partial or whole brain RT and in more than 50% at 6 months (8). RICD is particularly important in patients with low grade and benign tumors who are expected to have long-term survivals. In these patients, treatment selection to maximize quality of life and minimize cognitive deficits is imperative. Considerable efforts have been directed toward understanding and preventing radiation-induced cognitive decline (RICD), an important late effect of radiation therapy (5, 9, 10). To date, multiple mechanisms underlying RICD have been elucidated, including damage to sites of neurogenesis (11, 12), neuroinflammation (13, 14), neuronal dysfunction (15), and vascular changes (16-18).

RICD can occur in the absence of any gross anatomical changes. Advanced magnetic resonance imaging (MRI) techniques, however, may be able to detect effects from RT early on and may help elucidate mechanisms of radiation damage in RICD (19). MRI can examine volumetric and connectivity changes (both functional and structural) as well as changes in brain vasculature and perfusion. MRI may ultimately provide tools to identify patients at risk for RICD and help to direct efforts to prevent or ameliorate cognitive decline. Accordingly, accurate modeling of neurocognitive function with neuropsychological tests and correlation with *in vivo* imaging findings may help to identify putative biomarkers for routine quantitative evaluation of cognitive changes in patients with RICD. Novel MRI biomarkers of RICD are essential to improve understanding of how RT affects the brain structurally and functionally, to identify potential targets and therapeutics to mitigate RICD, and to improve initial RT plans to decrease complication rates.

RT affects both gray and white matter structures, yet the functional implications of these changes are actively being investigated. Studies have shown that cranial RT is associated with dose-dependent atrophy of the cortex (20), hippocampus (21) and amygdala (22) on T1-weighted (T1w) MRI. The hippocampus in particular has garnered attention as a vulnerable structure in the setting of RT; where RT has been shown to reduce neurogenesis (23, 24) and the pool of neural stem cells in the dentate gyrus (25, 26). Additionally, radiation dose to the hippocampus has also been shown to predict Hopkins Verbal Learning Test scores after brain irradiation (27). **Currently, the hippocampus is the only intracranial structure for which validated dose constraints are used in standard treatment planning (28-31).** NRG Oncology CC001 showed that conformal avoidance of the bilateral hippocampi (important structures in learning and memory) during whole brain RT reduced the risk of cognitive decline at 6 months from 68.2% to 59.5% (32). Despite advances in understanding of the role of the hippocampus in RICD, however, nearly 60% of patients still experience diminished cognitive function after RT despite conformal avoidance of the hippocampus. Moreover, recent studies have shown that radiation dose to the corpus callosum and surrounding white matter tracts can impact attention and processing speed at 6 months post-RT (33), executive function with radiation damage to the anterior cingulate cortex (34), damage to perisylvian white matter can predict language dysfunction (35), and damage to the hippocampus, temporal pole, and entorhinal cortex can predict changes in visuospatial memory (36). Thus, while the hippocampus is undoubtedly an important structure in memory formation, the singular focus on this region likely belies the complexity of structures and networks involved in memory formation and ignores the contribution of other anatomic structures to cognitive deficits seen post-therapy.

**Novelty and Innovation:** While there have been some strides made in understanding RICD, there remain significant gaps in our knowledge, which our study hopes to address. These include applications of rs-fMRI in prediction of RICD, evaluation of cognitive outcomes after hypofractionated radiation for low grade and benign brain tumors, evaluation of novel areas of interest that could contribute to cognitive decline, and integration of established autosegmentation software such as Freesurfer with radiation dose information.

Whole brain networks can be evaluated by analyzing structural and functional connections within the brain and their connections to function and behavior (37). Structural connectivity in the brain is measured by tracing white matter tracts derived from diffusion tensor imaging (DTI), (38). DTI evaluates the direction and magnitude of water molecular diffusion in a three-dimensional space (diffusion tensor) and can provide information on anisotropic diffusion. Additional quantitative metrics such as the fractional anisotropy (FA), axial diffusivity (AD), mean diffusivity (MD), and radial diffusivity (RD) can be obtained from DTI and can help describe different disease states such as demyelination (39, 40). Studies using DTI have shown that RT results in atrophy, demyelination of white matter, and gliosis (41) particularly in patients with a history of demyelinating diseases (42). Partial brain RT has also been shown to result in decreased AD and increased RD within the parahippocampal cingulum, where these changes are correlated with declines in verbal memory and fluency (43). Notably, reconstruction of fiber tracts in brain tumors and surrounding tissues is confounded by false continuities within the tumor and surrounding edema (44). Accordingly, advanced diffusion methods have recently been developed to model and eliminate free water with single-shell diffusion weighted imaging data, to more accurately model the tissue microstructure of surrounding normal brain tissue (45). However, similar to gross volumetric changes, apparent evidence of white matter atrophy and demyelination may not be discernable prior to 6 months or 1-year post-RT (46, 47). Resting state functional MRI (rs-fMRI) can be used to evaluate functional connectivity. In particular, graph-theory analysis of functional connectivity has revealed topological organization of brain networks (48), which has been used to investigate how network topology is affected in development (49), aging (50) and pathology (51-53). Graph theory-based approaches treat the brain as a network of nodes and edges, where nodes can be a region of interest (ROI) or a single voxel. Edges are the connections between each node. These graphical relationships can then be modeled as a correlation matrix, in which cross correlation is performed to determine the strength between pairs of nodes. Analysis of these matrices has revealed the brain to be highly modular (54, 55), with specific network hubs (areas of many connections to other nodes)(56), which have been shown to change in the setting of pathology and RT (57). Nevertheless, it is not known whether functional network changes can predict RICD or precede structural changes on MRI.

There has been limited evaluation of whether rs-fMRI can be used to predict early radiation changes. This may be partially due to difficulty in using rs-fMRI in high grade glioma (33). Other studies have consistently demonstrated that IDH wild type gliomas (ie. gliomas with more aggressive histology) have greater impact on functional connectivity metrics such as global functional connectivity derived from rs-fMRI (58) as well as impact baseline cognitive status to a greater degree prior to any treatment (59). When limited to select patients, this modality may be useful as an MRI biomarker in early grade and benign brain tumor patients receiving radiation. Further studies focused on that population and excluding high grade glioma patients, such as this one, are needed. Whole brain metrics such as functional connectivity may provide early identification of subjects who are at risk of decline and can be targeted with novel therapeutics. Preliminary studies are limited but suggest that rs-fMRI and functional connectivity represent a promising modality with which to develop dose constraints and mitigate cognitive decline after RT (60-62).

**Study Aims:** Investigation into structures outside the hippocampus that can be spared in order to improve cognitive outcomes remains an area of active study. We have the most data for RICD related

to radiation dose to the corpus callosum (33, 63) and hippocampus (31, 32). However, we currently have no valid dose constraints for the structures outside the hippocampus including the corpus callosum. Development of dose constraints and investigation of which structures can be avoided and lead to improvement in clinical outcomes is an area of active research as we seek to understand the complex structural and functional relationships that lead to RICD (64).

Additionally, radiosurgery and fractionated radiosurgery are important modalities used frequently in the treatment of benign brain tumors. With the increased use of hypofractionation and radiosurgery, it is important to establish dose constraints that are valid in the setting of high dose per fraction (65). As of now, we have little data on dose constraints for cognitive avoidance structures in the setting of hypofractionation, and much is extrapolated from studies of conventional fractionation.

Accordingly, this study will evaluate the effects of RT in patients with benign and low-grade brain tumors using multimodal neuroimaging and a battery of neurocognitive tests. We hypothesize that radiation induced damage will manifest prior to gross anatomical changes via alterations in network topology and microstructural integrity. Ultimately, we aim to establish structures beyond the hippocampus that are vulnerable to RT and develop dose constraints to minimize the risk and progression of RICD in this vulnerable patient population.

## METHODS and ANALYSIS

### Study Design

A total of 75 patients with benign and low-grade brain tumors planned to receive partial brain RT, either hypofractionated (>2 Gy/fraction) or conventionally fractionated (1.8-2 Gy/fraction), will be enrolled at the Wilmot Cancer Institute. All participants provide written informed consent according to the Institutional Review Board (IRB) approved protocol prior to any evaluation. Subjects are followed for 12 months.

Key inclusion criteria include 1) age ≥18-years; 2) patients with benign or low-grade brain tumors including low grade gliomas, meningiomas, acoustic neuromas, pituitary adenomas, craniopharyngiomas, hemangiopericytomas, or other benign or low-grade brain tumors; 3) planned to receive either conventional or hypofractionated RT; 4) no contraindication to gadolinium-enhanced MRI. Surgical excision and/or chemotherapy prior to enrollment is permitted.

Key exclusion criteria include 1) Prior cranial RT; 2) Inability to participate in neurocognitive testing; 3) Intractable seizures; 4) Non-English speaking; 5) Aphasia limiting ability to participate in neurocognitive testing.

Subjects will undergo three comprehensive evaluations (baseline, 6-month, and 12-month time points) that include clinical evaluation, MRI, a battery of neurocognitive tests, and questionnaires which evaluate patient-reported cognition, fatigue, anxiety, and depression. An additional 3-month timepoint includes questionnaires and neurocognitive testing only (Figure 1).

### Patient and Public Involvement

Patients will be involved in the design and conduct of this research. After completion of this pilot cohort study, we will plan to further tailor the study design for a larger study by conducting interviews with participants. Once the trial has been published, participants will be informed of the results via email.

**Neurocognitive Testing**

Assessments of neurocognitive and functional performance are performed to evaluate neurocognitive changes post-RT. The components of the neurocognitive testing battery are described in Table 1. The battery includes the standard tests recommended by the International Cognition and Cancer Task Force (66) testing verbal memory (HVLT-R, (67, 68), verbal fluency (COWA, (69), and executive function (TMT(70, 71). However, the battery additionally includes the BVMT-R, which has a similar format to the HVLT-R but focuses on visuospatial learning and memory (36), as well as additional iPad-based tests from Cambridge Cognition which have been shown to be valid and sensitive in the assessment of cancer-related cognitive impairment (72-74). Neuropsychological testing is administered by trained study coordinators using a standardized testing manual; study coordinators are supervised by the study team with expertise in neurology, neuropsychology and cognitive science. Raw scores will be used in analysis and adjusted for covariates such as age. Testing is performed in a quiet, comfortable room without distractions.

**Table 1.** Description and platform of tests in cognitive battery

| Test | Description | Cognitive Domain | Platform |
|---|---|---|---|
| **Wide Range Achievement Test-4 (WRAT-4)** | Word reading | Cognitive reserve, education level | Paper-based |
| **Hopkins Verbal Learning Test-Revised (HVLT-R)** | Immediate and delayed recall of a word list | Verbal learning and memory | Paper-based |
| **Controlled Oral Word Associated Test (COWA)** | Number of words the subject can provide in a category over one minute | Verbal fluency | Paper-based |
| **Trailmaking Test A and B (TMT-A and TMT-B)** | Connect circles containing a series of numbers (A) or numbers and letters (B) in a pattern | Executive function | Paper-based |
| **Brief Visuospatial Memory Test-Revised (BVMT-R)** | Immediate and delayed recall of a series of shapes and designs | Visuospatial learning and memory | Paper-based |
| **Emotional Recognition Task (ERT)** | Identification of the emotion indicated by a facial expression | Emotional and social cognition | Cambridge cognition |
| **Spatial Working Memory (SWM)** | Use of strategy to find a yellow token behind colored boxes | Executive function, visuospatial working memory | Cambridge cognition |
| **Paired Associates Learning (PAL)** | Match the pattern to the box where it was previously displayed | Visuospatial episodic memory and new learning | Cambridge cognition |
| **Delayed Matching to Sample (DMS)** | Matching of complex visual patterns | Visual matching ability and short-term visual recognition memory | Cambridge cognition |
| **Reaction Time Task (RTT)** | Select a circle in which a yellow dot appears | Assessment of motor and mental response speed | Cambridge cognition |

**Patient Reported Outcomes**

Patient reported outcome measures of symptoms that may influence cognition are recorded longitudinally so that they can be studied and accounted for in analyses. These symptoms include fatigue, anxiety, and depression using validated measures including the Functional Assessment of Cancer Therapy-Brain (FACT-Br, neurologic symptoms in brain tumor patients, (75), Functional Assessment of Cancer-Fatigue (FACIT-Fatigue, symptoms of fatigue, (76), Patient Health Questionnaire-9 (PHQ-9, symptoms of depression, (77), State-Trait Anxiety Inventory (STAI, (78), and Short Form of the Profile of Mood States-2 (POMS2-SF, subscales of anger-hostility, confusion-bewilderment, depression-dejection, fatigue-inertia, tension-anxiety, vigor-activity, and friendliness, (79). Subjective cognition is measured using the Functional Assessment of Cancer Therapy-Cognition (FACT-COG, (80) for comparison with scores on objective neurocognitive testing.

**Demographic and Clinical Information**

Patient characteristics that may affect cognitive outcomes and trajectories are recorded, including age, education level, comorbidities including diabetes, hypertension, autoimmune disease, tumor hemisphere, tumor site, tumor pathology, prior surgeries, employment status, smoking status, alcohol use, sex/gender, hypopituitarism, menopausal status, steroid use, use of medications that can affect cognition and mood, and exposure to chemotherapy.

**Radiotherapy Planning**

Each patient is planned and treated per standard of care by their treating radiation oncologist. RT plans for single fraction or fractionated radiosurgery are created using BrainLAB Elements® planning software. All other plans were created using Varian Eclipse® treatment planning software. For consistency, all radiation dose maps were calculated in Eclipse for all patients using a 1 mm x 1 mm grid.

**MRI Acquisition**

All imaging is performed on a 3T GE Discovery 750 MRI system (Milwaukee, WI, USA), equipped with an 8-channel head coil. High-resolution T1w anatomical images are acquired using a 3D BRAVO FSPGR sequence with the following parameters: repetition time (TR)= 8.2 ms, echo time (TE)= 3.2 ms, field of view (FOV) 256 $mm^2$, resolution 1x1x1$mm^3$.

Blood oxygen level dependent (BOLD) rs-fMRI is acquired using a BOLD sensitive gradient-echo echo planar imaging (GE-EPI) sequence with the following parameters: TR=2000ms, TE=30ms, FOV=192$mm^2$, resolution 3x3x3 $mm^3$, 150 volumes.

In order to evaluate white matter integrity and microstructural changes, we make use of a standard clinical DTI protocol with 30 diffusion directions, demonstrated to be sufficient for reconstructing white matter fiber tracts and not to affect test-retest reliability (81). DTI is acquired using a 2D axial single-shot dual spin-echo EPI (SE-EPI) sequence with the following parameters: TR= 10,000ms, TE= 81ms, FOV=256$mm^2$, resolution 2x2x2 $mm^3$, 30 diffusion weighted directions with b=1000s/$mm^2$ and 4 b=0 reference images.

**MRI Data Processing**

Herein we describe a comprehensive image analysis pipeline, which includes preprocessing, data cleaning, and post-processing for each imaging modality, including advanced modelling and calculation of quantitative imaging biomarkers (Figure 2).

All image processing is completed within URMC servers in the Center for Integrated Research Computing (CIRC), using BHWARD, a HIPAA compliant server.

**RT Dose Calculations**

The RT dose map is first scaled and mapped with CT images using pydicom (version 1.4). T1w images are registered to subject-specific CT space using FMRIB's Linear Image Registration Tool (FLIRT, (82). Subject specific parcellations derived from the Desikan-Killiany (83) atlas using Freesurfer are registered with the RT dose map. The mean, maximum, and minimum RT doses are extracted from each ROI, and the 2 Gy/fraction equivalent dose (EQD2) is calculated using the linear quadratic model (84), with an $\alpha/\beta$ equal to 3, to model the radiosensitivity of normal brain tissue (85).

**T1w**

T1w images are processed by first masking out the tumor using the gross target volume (GTV) as contoured by the primary radiation oncologist from the RT structure set (86), delineated on planar MRI and CT imaging, using nibabel (https://nipy.org, version 3.1.1). This is achieved by mapping the GTV to the CT images in subject space, and then performing an affine transform to register the T1-w images to the subject specific CT images (Figure 3). Thereafter, segmentation is performed using the tumor masked T1-w in Freesurfer (version 6.0.0, http://surfer.nmr.harvard.edu). The Freesurfer pipeline is run independently for each subject at each time point (pre-RT, 6-months, and 12-months post-RT). Briefly, processing includes skull-stripping and removal of non-brain tissue, motion correction, intensity normalization, automated Talairach transformation, white matter segmentation, and cortical parcellation using the Desikan-Killiany atlas (83), which includes cortical and subcortical regions of interest (ROIs). Subsequent segmentation of thalamic nuclei was also performed using a probabilistic atlas based on ex vivo MRI and histology (87).

**Diffusion Imaging**

DTI data is pre-processed using FMRIB's Software Library (FSL, (88-91) diffusion toolbox (FDT, http://fsl.fmrib.ox.ac.uk/fsl). Briefly, inter-volume subject motion, brain extraction using BET (91), and eddy-current induced distortion correction are performed using EDDY (92). The diffusion tensors are then fit on eddy-corrected data using DTIFIT (93). DTIFIT fits a diffusion tensor model at each voxel and provides the 3 principal eigenvectors and eigenvalues of the diffusion tensor, from which the fractional anisotropy (FA), mean diffusivity (MD), axial diffusivity (AD), and radial diffusivity (RD) can be measured (93). All images are then registered to MNI standard space and interpolated to 1 $mm^3$ voxels. Binary gross target volume masks are then used to mask out abnormal tissue in processed maps. The JHU white-matter tractography atlas, composed of 20 structures identified using probabilistic tractography, is then used to extract mean FA, MD, AD, and RD values from regions of interest (94).

**Functional Imaging**

rs-fMRI data is processed using FSL's FMRI Expert Analysis Tool (FEAT, version 6.00)(95). Registration to high resolution structural space is carried out using a two-stage registration. First rs-fMRI data is registered to high-resolution structural space using FMRIB's Linear Image Registration Tool (FLIRT, (82), and then registration to MNI standard space (96) is further refined using FMRIB's Nonlinear Image Registration Tool (FNIRT, (97). Since field maps were not acquired as part of the clinical scan protocol, a 12 degrees-of-freedom affine transformation was used for linear and nonlinear registration. All registrations are visually inspected during processing. Further preprocessing includes skull stripping using BET (91), motion correction using MCFLIRT (82), slice-time correction, spatial smoothing using a Gaussian kernel of FWHM 5mm, and high-pass temporal filtering.

Single-session independent component analysis (ICA) is then performed for each subject using probabilistic ICA implemented in FSL's Multivariate Exploratory Linear Optimized Decomposition into Independent Components (MELODIC, Version 3.15). MELODIC de-composes input data into separate time courses and spatial maps using probabilistic principal component analysis (PCA). FMRIB's ICA-based Xnoisifier (FIX, (98, 99) is then used to further denoise functional data by automatically classifying signal versus noise components from the time series data. FIX is run using the standard pre-trained data (TR=3s, 3.5x3.5x3.5mm resolution, 6 minutes) which was preprocessed using default FEAT processing. All images and components are visually inspected for accuracy prior to further processing.

Once all fMRI data has been preprocessed, the denoised functional data is used to construct subject specific functional connectivity (FC) matrices. Subject specific atlases generated using Freesurfer are then registered to the MNI standard space and used to extract the mean time series from each ROI. This is done to ensure that only functional regions outside of the tumor are used to construct FC matrices. FC matrices are then generated by computing the cross correlation between all pairs of nodes (ROIs), using the Pearson correlation coefficient (Figure 4).

Subject specific FC matrices are then analyzed using the Brain Connectivity Toolbox (100) in MATLAB (R2020a). Subject specific correlation matrices are thresholded to yield weighted undirected networks, and analyzed using graph theory to yield measures of functional integration and segregation. Global measures of integration, including global efficiency, transitivity and modularity, are then computed for further statistical analysis (101). Local measures of segregation, including clustering coefficient and local efficiency (Table 2), are also computed for each ROI for further statistical analysis. A more thorough review of graph theory-based measures for rs-fMRI may be found in Rubinov and Sporns, 2010 (102).

**Table 2.** Overview of graph theory measures used to analysis resting state functional connectivity and structural connectivity obtained from diffusion tractography. A more in depth review of graph theory and graph theory measures can be found in Rubinov and Sporns, 2010 (93)

| Measurement | Definition | Equation |
|---|---|---|
| **Node Degree** | The number of connections between one node and the rest of the network | $k_i = \Sigma(a_{ij})$ |
| **Clustering Coefficient** | The number of connections between the neighbors of a node. | $2t/(k(k-1))$; k is the node degree; t is the fraction of triangles around a node. |
| **Efficiency** | Inverse of path length (minimum number of edges to traverse from one node to another) | $\frac{1}{N(N-1)}\Sigma\left(\frac{1}{d_{ij}}\right)$ Where $d_{ij}$ is the shortest path length between nodes i and j |
| **Modularity** | Areas of highly interconnected nodes, with few connections to nodes in other modules. | $Q = \frac{1}{l}\Sigma\left(a_{ij} - \frac{(k_i k_j)}{l}\right)\delta(m_i, m_j)$ |

**Power & Sample Size Justification**

We estimate that 52 evaluable patients (a total of 75 subjects allowing for 30% of subjects with missing or incomplete data) will have ≥80% power to detect at least 0.4 standard deviation (SD) change on the delayed recall measure of the HVLT-R post-RT. The power analysis is based on a paired t-test with a two-sided significance level of 0.05.

**Analysis Plan**

Graphical methods will be used to explore the cognitive test and imaging data, to visually describe and compare distributions of continuous variables, and to visualize results of statistical analyses. Quantitative imaging metrics (cortical thickness, subcortical volume, FA, MD, AD, RD, local efficiency, and clustering coefficient) will be analyzed to investigate their relationships with RT dose and cognitive measures. Comparisons between raw scores on cognitive tests and imaging metrics pre and post-RT will be performed using paired t-tests and Wilcoxon signed-rank tests. Pearson and Spearman correlation analyses will be used to assess associations between pairs of continuous measures. Multivariate mixed effect regression models will be used to evaluate the relationships of cognitive tests at 6-month and 12-month visits with RT dose adjusting for the baseline cognitive test, imaging parameters, age, gender, tumor laterality, and tumor type. During the analyses, false discovery rate (FDR) method will be used to account for multiple comparisons (103). All statistical analyses will be performed using R (R Foundation for Statistical Computing, Vienna, Austria) or SAS 9.4.

## DISCUSSION & CONCLUSION

RICD is an important target of efforts to use more sophisticated radiation techniques such as intensity modulated radiation therapy and proton therapy in order to decrease side effects (104). While validated dose constraints exist for structures such as the brainstem, cochlea, optic nerves and chiasm, and pituitary gland (28), development of dose constraints for intracranial structures involved in cognition is a new and exciting area of research that promises to improve radiation outcomes. Despite conformal dose reduction to the hippocampi, RICD occurs in a large percentage of patients, reflecting the complexity of memory formation and the need to identify non-hippocampal structures involved in higher cognitive functions. The pathology underlying RICD likely begins prior to any gross anatomical changes or noticeable differences in cognition observed by the patient. Accordingly, development of quantitative in vivo biomarkers is essential for developing dose constraints and monitoring RICD.

This study utilizes conventional and advanced MRI, neurocognitive testing, and dosimetry information to provide a comprehensive description of RICD in patients with brain tumors receiving radiation therapy. The proposed analyses will provide insight into which intracranial structures are particularly susceptible to RT and how they modulate changes in cognition via aberrant network topology. The results of this study will help to provide dose constraints to better avoid cognitive decline that can ultimately be used to create radiation plans associated with less cognitive change. Incorporation of rs-fMRI into treatment planning and monitoring has the potential to improve cognitive outcomes in the setting of RT and provide personalized treatment. Additionally, utilization of graph theory will be able to identify specific nodes and hubs within brain networks that are susceptible to RT at the population and individual level (105).

This protocol and analysis pipeline will aid researchers interested in combining MRI imaging data including segmentation of intracranial structures not used in standard radiation planning with radiation dosimetry information to advance our understanding of RICD. We provide detailed information on study design, clinical and imaging protocols and analysis pipeline with which to investigate RT-induced cognitive changes on intracranial structures that are not segmented with standard radiation planning software. This is an important and complex process which should be

transparent, and one of our goals with this paper is to promote utilization of open software packages in a useful and standardized way for the radiation oncology community.

## ETHICS AND DISSEMINATION

Studies involving human participants were reviewed and approved by the University of Rochester Subjects Review Board. All patients/participants provided their written informed consent to participate in this study. All results will be presented at relevant conferences and published in relevant peer-reviewed journals.

## AUTHOR CONTRIBUTIONS

Sara J Hardy: Protocol development and design, principal investigator, manuscript editing
Alan Finkelstein: Development of MRI pipeline for processing and analysis, manuscript editing
Eva Culakova: Development of statistical plan and power analysis, manuscript editing
Kenneth Usuki: Mentorship on clinical aspects of protocol and recruitment, manuscript editing
Jianhui Zhong: MRI protocol development, manuscript editing
Michelle Janelsins: Research mentorship in cognitive assessment, help with protocol development, manuscript editing
Giovanni Schifitto: Research mentorship in neuroimaging, help with protocol development and manuscript editing
Michael Milano: Research mentorship in evaluation of radiation toxicity, help with protocol development and manuscript editing
Nimish Mohile: Research mentorship in neuro-oncology, help with protocol development and manuscript editing
Madalina Tivarus: MRI protocol development, manuscript editing
Edward Lin: MRI protocol development, manuscript editing
Miriam Weber: Clinical neuropsychology, development of cognitive battery and interpretation of cognitive data, manuscript editing

## FUNDING

This work is supported by the Department of Radiation Oncology (internal funding), Schmitt Foundation Grant number GR505052 (PI: Hardy), DP2 grant number DP2195765 (PI: Michelle Janelsins), R01MH118020 and R01AG054328 (PI: Schifitto), and the Wilmot Cancer Research Fellowship and Cancer Control T32 grant number CA102618, The project described in this publication was also supported by the University of Rochester CTSA award number UL1TR002001 from the National Center for Advancing Translational Sciences of the National Institutes of Health. The content is solely the responsibility of the authors and does not necessarily represent the official views of the National Institutes of Health.

## CONFLICT OF INTEREST STATEMENT

The authors declare that the research was conducted in the absence of any commercial or financial relationships that could be construed as a potential conflict of interest.

## ACKNOWLEDGEMENTS

Support from the Department of Radiation Oncology at University of Rochester

## REFERENCES

1. Taphoorn MJ, Klein M. Cognitive deficits in adult patients with brain tumours. Lancet Neurol. 2004;3(3):159-68.
2. Klaver KM, Duijts SFA, Engelhardt EG, Geusgens CAV, Aarts MJB, Ponds R, et al. Cancer-related cognitive problems at work: experiences of survivors and professionals. J Cancer Surviv. 2020;14(2):168-78.
3. Harrison RA, Wefel JS. Neurocognitive Function in Adult Cancer Patients. Neurol Clin. 2018;36(3):653-74.
4. Salans M, Tibbs MD, Huynh-Le MP, Yip A, Tringale K, Karunamuni R, et al. Quality of Life Is Independently Associated With Neurocognitive Function in Patients With Brain Tumors: Analysis of a Prospective Clinical Trial. Int J Radiat Oncol Biol Phys. 2021;111(3):754-63.
5. Pazzaglia S, Briganti G, Mancuso M, Saran A. Neurocognitive Decline Following Radiotherapy: Mechanisms and Therapeutic Implications. Cancers (Basel). 2020;12(1).
6. Hardy SJ, Krull KR, Wefel JS, Janelsins M. Cognitive Changes in Cancer Survivors. Am Soc Clin Oncol Educ Book. 2018;38:795-806.
7. Coomans MB, van der Linden SD, Gehring K, Taphoorn MJB. Treatment of cognitive deficits in brain tumour patients: current status and future directions. Curr Opin Oncol. 2019;31(6):540-7.
8. Makale MT, McDonald CR, Hattangadi-Gluth JA, Kesari S. Mechanisms of radiotherapy-associated cognitive disability in patients with brain tumours. Nat Rev Neurol. 2017;13(1):52-64.
9. Greene-Schloesser D, Moore E, Robbins ME. Molecular pathways: radiation-induced cognitive impairment. Clin Cancer Res. 2013;19(9):2294-300.
10. Greene-Schloesser D, Robbins ME. Radiation-induced cognitive impairment--from bench to bedside. Neuro Oncol. 2012;14 Suppl 4:iv37-44.
11. Michaelidesova A, Konirova J, Bartunek P, Zikova M. Effects of Radiation Therapy on Neural Stem Cells. Genes (Basel). 2019;10(9).
12. Bellinzona M, Gobbel GT, Shinohara C, Fike JR. Apoptosis is induced in the subependyma of young adult rats by ionizing irradiation. Neurosci Lett. 1996;208(3):163-6.
13. Lumniczky K, Szatmari T, Safrany G. Ionizing Radiation-Induced Immune and Inflammatory Reactions in the Brain. Front Immunol. 2017;8:517.
14. Constanzo J, Midavaine E, Fouquet J, Lepage M, Descoteaux M, Kirby K, et al. Brain irradiation leads to persistent neuroinflammation and long-term neurocognitive dysfunction in a region-specific manner. Prog Neuropsychopharmacol Biol Psychiatry. 2020;102:109954.
15. Wu PH, Coultrap S, Pinnix C, Davies KD, Tailor R, Ang KK, et al. Radiation induces acute alterations in neuronal function. PLoS One. 2012;7(5):e37677.
16. Weintraub NL, Jones WK, Manka D. Understanding radiation-induced vascular disease. J Am Coll Cardiol. 2010;55(12):1237-9.
17. Venkatesulu BP, Mahadevan LS, Aliru ML, Yang X, Bodd MH, Singh PK, et al. Radiation-Induced Endothelial Vascular Injury: A Review of Possible Mechanisms. JACC Basic Transl Sci. 2018;3(4):563-72.

18. Venkatesulu BP, Sanders KL, Hsieh CE, Kim BK, Krishnan S. Biomarkers of radiation-induced vascular injury. Cancer Rep (Hoboken). 2019;2(2):e1152.
19. Greene-Schloesser D, Robbins ME, Peiffer AM, Shaw EG, Wheeler KT, Chan MD. Radiation-induced brain injury: A review. Front Oncol. 2012;2:73.
20. Karunamuni R, Bartsch H, White NS, Moiseenko V, Carmona R, Marshall DC, et al. Dose-Dependent Cortical Thinning After Partial Brain Irradiation in High-Grade Glioma. Int J Radiat Oncol Biol Phys. 2016;94(2):297-304.
21. Seibert TM, Karunamuni R, Bartsch H, Kaifi S, Krishnan AP, Dalia Y, et al. Radiation Dose-Dependent Hippocampal Atrophy Detected With Longitudinal Volumetric Magnetic Resonance Imaging. Int J Radiat Oncol Biol Phys. 2017;97(2):263-9.
22. Huynh-Le MP, Karunamuni R, Moiseenko V, Farid N, McDonald CR, Hattangadi-Gluth JA, et al. Dose-dependent atrophy of the amygdala after radiotherapy. Radiother Oncol. 2019;136:44-9.
23. Kang J, Kim W, Seo H, Kim E, Son B, Lee S, et al. Radiation-induced overexpression of transthyretin inhibits retinol-mediated hippocampal neurogenesis. Sci Rep. 2018;8(1):8394.
24. Ji S, Ding X, Ji J, Wu H, Sun R, Li X, et al. Cranial irradiation inhibits hippocampal neurogenesis via DNMT1 and DNMT3A. Oncol Lett. 2018;15(3):2899-904.
25. Ben Abdallah NM, Slomianka L, Lipp HP. Reversible effect of X-irradiation on proliferation, neurogenesis, and cell death in the dentate gyrus of adult mice. Hippocampus. 2007;17(12):1230-40.
26. Mineyeva OA, Bezriadnov DV, Kedrov AV, Lazutkin AA, Anokhin KV, Enikolopov GN. Radiation Induces Distinct Changes in Defined Subpopulations of Neural Stem and Progenitor Cells in the Adult Hippocampus. Front Neurosci. 2018;12:1013.
27. Okoukoni C, McTyre ER, Ayala Peacock DN, Peiffer AM, Strowd R, Cramer C, et al. Hippocampal dose volume histogram predicts Hopkins Verbal Learning Test scores after brain irradiation. Adv Radiat Oncol. 2017;2(4):624-9.
28. Scoccianti S, Detti B, Gadda D, Greto D, Furfaro I, Meacci F, et al. Organs at risk in the brain and their dose-constraints in adults and in children: a radiation oncologist's guide for delineation in everyday practice. Radiother Oncol. 2015;114(2):230-8.
29. Kazda T, Jancalek R, Pospisil P, Sevela O, Prochazka T, Vrzal M, et al. Why and how to spare the hippocampus during brain radiotherapy: the developing role of hippocampal avoidance in cranial radiotherapy. Radiat Oncol. 2014;9:139.
30. Gondi V, Tolakanahalli R, Mehta MP, Tewatia D, Rowley H, Kuo JS, et al. Hippocampal-sparing whole-brain radiotherapy: a "how-to" technique using helical tomotherapy and linear accelerator-based intensity-modulated radiotherapy. Int J Radiat Oncol Biol Phys. 2010;78(4):1244-52.
31. Gondi V, Tome WA, Mehta MP. Why avoid the hippocampus? A comprehensive review. Radiother Oncol. 2010;97(3):370-6.
32. Gondi V, editor Preservation of Neurocognitive Function with Conformal Avoidance of the Hippocampus during Whole-Brain Radiotherapy for Brain Metastases: Preliminary Results of Phase III Trial NRG Oncology CC001. Annual Meeting of the American Society for Radiation Oncology; 2018; San Antonio, TX.
33. Huynh-Le MP, Tibbs MD, Karunamuni R, Salans M, Tringale KR, Yip A, et al. Microstructural Injury to Corpus Callosum and Intrahemispheric White Matter Tracts Correlate With Attention and Processing Speed Decline After Brain Radiation. Int J Radiat Oncol Biol Phys. 2021;110(2):337-47.
34. Tringale KR, Nguyen T, Bahrami N, Marshall DC, Leyden KM, Karunamuni R, et al. Identifying early diffusion imaging biomarkers of regional white matter injury as indicators of executive function decline following brain radiotherapy: A prospective clinical trial in primary brain tumor patients. Radiother Oncol. 2019;132:27-33.

35. Tibbs MD, Huynh-Le MP, Karunamuni R, Reyes A, Macari AC, Tringale KR, et al. Microstructural Injury to Left-Sided Perisylvian White Matter Predicts Language Decline After Brain Radiation Therapy. Int J Radiat Oncol Biol Phys. 2020;108(5):1218-28.
36. Tringale KR, Nguyen TT, Karunamuni R, Seibert T, Huynh-Le MP, Connor M, et al. Quantitative Imaging Biomarkers of Damage to Critical Memory Regions Are Associated With Post-Radiation Therapy Memory Performance in Brain Tumor Patients. Int J Radiat Oncol Biol Phys. 2019;105(4):773-83.
37. Sporns O, Tononi G, Kotter R. The human connectome: A structural description of the human brain. PLoS Comput Biol. 2005;1(4):e42.
38. Baliyan V, Das CJ, Sharma R, Gupta AK. Diffusion weighted imaging: Technique and applications. World J Radiol. 2016;8(9):785-98.
39. Tournier JD, Mori S, Leemans A. Diffusion tensor imaging and beyond. Magn Reson Med. 2011;65(6):1532-56.
40. Le Bihan D, Mangin JF, Poupon C, Clark CA, Pappata S, Molko N, et al. Diffusion tensor imaging: concepts and applications. J Magn Reson Imaging. 2001;13(4):534-46.
41. Wang S, Wu EX, Qiu D, Leung LH, Lau HF, Khong PL. Longitudinal diffusion tensor magnetic resonance imaging study of radiation-induced white matter damage in a rat model. Cancer Res. 2009;69(3):1190-8.
42. Milic M, Rees JH. Acute demyelination following radiotherapy for glioma: a cautionary tale. Pract Neurol. 2017;17(1):35-8.
43. Chapman CH, Zhu T, Nazem-Zadeh M, Tao Y, Buchtel HA, Tsien CI, et al. Diffusion tensor imaging predicts cognitive function change following partial brain radiotherapy for low-grade and benign tumors. Radiother Oncol. 2016;120(2):234-40.
44. Henderson F, Abdullah KG, Verma R, Brem S. Tractography and the connectome in neurosurgical treatment of gliomas: the premise, the progress, and the potential. Neurosurg Focus. 2020;48(2):E6.
45. Parker D, Ould Ismail AA, Wolf R, Brem S, Alexander S, Hodges W, et al. Freewater estimatoR using iNtErpolated iniTialization (FERNET): Characterizing peritumoral edema using clinically feasible diffusion MRI data. PLoS One. 2020;15(5):e0233645.
46. Chapman CH, Nagesh V, Sundgren PC, Buchtel H, Chenevert TL, Junck L, et al. Diffusion tensor imaging of normal-appearing white matter as biomarker for radiation-induced late delayed cognitive decline. Int J Radiat Oncol Biol Phys. 2012;82(5):2033-40.
47. Nagesh V, Tsien CI, Chenevert TL, Ross BD, Lawrence TS, Junick L, et al. Radiation-induced changes in normal-appearing white matter in patients with cerebral tumors: a diffusion tensor imaging study. Int J Radiat Oncol Biol Phys. 2008;70(4):1002-10.
48. Bullmore E, Sporns O. Complex brain networks: graph theoretical analysis of structural and functional systems. Nat Rev Neurosci. 2009;10(3):186-98.
49. Suprano I, Delon-Martin C, Kocevar G, Stamile C, Hannoun S, Achard S, et al. Topological Modification of Brain Networks Organization in Children With High Intelligence Quotient: A Resting-State fMRI Study. Front Hum Neurosci. 2019;13:241.
50. Varangis E, Habeck CG, Razlighi QR, Stern Y. The Effect of Aging on Resting State Connectivity of Predefined Networks in the Brain. Front Aging Neurosci. 2019;11:234.
51. Openneer TJC, Marsman JC, van der Meer D, Forde NJ, Akkermans SEA, Naaijen J, et al. A graph theory study of resting-state functional connectivity in children with Tourette syndrome. Cortex. 2020;126:63-72.

52. Khazaee A, Ebrahimzadeh A, Babajani-Feremi A. Identifying patients with Alzheimer's disease using resting-state fMRI and graph theory. Clin Neurophysiol. 2015;126(11):2132-41.
53. Sjoerds Z, Stufflebeam SM, Veltman DJ, Van den Brink W, Penninx BW, Douw L. Loss of brain graph network efficiency in alcohol dependence. Addict Biol. 2017;22(2):523-34.
54. Caparelli EC, Ross TJ, Gu H, Liang X, Stein EA, Yang Y. Graph theory reveals amygdala modules consistent with its anatomical subdivisions. Sci Rep. 2017;7(1):14392.
55. Meunier D, Lambiotte R, Fornito A, Ersche KD, Bullmore ET. Hierarchical modularity in human brain functional networks. Front Neuroinform. 2009;3:37.
56. Power JD, Schlaggar BL, Lessov-Schlaggar CN, Petersen SE. Evidence for hubs in human functional brain networks. Neuron. 2013;79(4):798-813.
57. Bahrami N, Seibert TM, Karunamuni R, Bartsch H, Krishnan A, Farid N, et al. Altered Network Topology in Patients with Primary Brain Tumors After Fractionated Radiotherapy. Brain Connect. 2017;7(5):299-308.
58. Derks J, Kulik S, Wesseling P, Numan T, Hillebrand A, van Dellen E, et al. Understanding cognitive functioning in glioma patients: The relevance of IDH-mutation status and functional connectivity. Brain Behav. 2019;9(4):e01204.
59. Wefel JS, Noll KR, Rao G, Cahill DP. Neurocognitive function varies by IDH1 genetic mutation status in patients with malignant glioma prior to surgical resection. Neuro Oncol. 2016;18(12):1656-63.
60. Mitchell TJ, Seitzman BA, Ballard N, Petersen SE, Shimony JS, Leuthardt EC. Human Brain Functional Network Organization Is Disrupted After Whole-Brain Radiation Therapy. Brain Connect. 2020;10(1):29-38.
61. Duffau H. Why brain radiation therapy should take account of the individual structural and functional connectivity: Toward an irradiation "a la carte". Crit Rev Oncol Hematol. 2020;154:103073.
62. Li M, Zhang Q, Yang K. Role of MRI-Based Functional Imaging in Improving the Therapeutic Index of Radiotherapy in Cancer Treatment. Front Oncol. 2021;11:645177.
63. Redmond KJ, Hildreth M, Sair HI, Terezakis S, McNutt T, Kleinberg L, et al. Association of Neuronal Injury in the Genu and Body of Corpus Callosum After Cranial Irradiation in Children With Impaired Cognitive Control: A Prospective Study. Int J Radiat Oncol Biol Phys. 2018;101(5):1234-42.
64. Redmond KJ, Milano MT, Kim MM, Trifiletti DM, Soltys SG, Hattangadi-Gluth JA. Reducing Radiation-Induced Cognitive Toxicity: Sparing the Hippocampus and Beyond. Int J Radiat Oncol Biol Phys. 2021;109(5):1131-6.
65. Milano MT, Grimm J, Niemierko A, Soltys SG, Moiseenko V, Redmond KJ, et al. Single- and Multifraction Stereotactic Radiosurgery Dose/Volume Tolerances of the Brain. Int J Radiat Oncol Biol Phys. 2021;110(1):68-86.
66. Wefel JS, Vardy J, Ahles T, Schagen SB. International Cognition and Cancer Task Force recommendations to harmonise studies of cognitive function in patients with cancer. Lancet Oncol. 2011;12(7):703-8.
67. Shapiro AM, Benedict RH, Schretlen D, Brandt J. Construct and concurrent validity of the Hopkins Verbal Learning Test-revised. Clin Neuropsychol. 1999;13(3):348-58.
68. Rasmusson DX, Bylsma FW, Brandt J. Stability of performance on the Hopkins Verbal Learning Test. Arch Clin Neuropsychol. 1995;10(1):21-6.
69. Benton AL HK, Sivan AB. Controlled Oral Word Association Multilingual Aphasia Examination professional manual. Lutz, FL1978.
70. Gaudino EA, Geisler MW, Squires NK. Construct validity in the Trail Making Test: what makes Part B harder? J Clin Exp Neuropsychol. 1995;17(4):529-35.

71. Goul WR, Brown M. Effects of age and intelligence on trail making test performance and validity. Percept Mot Skills. 1970;30(1):319-26.
72. Janelsins MC, Heckler CE, Peppone LJ, Ahles TA, Mohile SG, Mustian KM, et al. Longitudinal Trajectory and Characterization of Cancer-Related Cognitive Impairment in a Nationwide Cohort Study. J Clin Oncol. 2018;36(32):Jco2018786624.
73. Fray PJ, Robbins TW. CANTAB battery: proposed utility in neurotoxicology. Neurotoxicol Teratol. 1996;18(4):499-504.
74. Robbins TW, James M, Owen AM, Sahakian BJ, McInnes L, Rabbitt P. Cambridge Neuropsychological Test Automated Battery (CANTAB): a factor analytic study of a large sample of normal elderly volunteers. Dementia. 1994;5(5):266-81.
75. Thavarajah N, Bedard G, Zhang L, Cella D, Beaumont JL, Tsao M, et al. Psychometric validation of the functional assessment of cancer therapy--brain (FACT-Br) for assessing quality of life in patients with brain metastases. Support Care Cancer. 2014;22(4):1017-28.
76. Minton O, Stone P. A systematic review of the scales used for the measurement of cancer-related fatigue (CRF). Ann Oncol. 2009;20(1):17-25.
77. Hinz A, Mehnert A, Kocalevent RD, Brähler E, Forkmann T, Singer S, et al. Assessment of depression severity with the PHQ-9 in cancer patients and in the general population. BMC Psychiatry. 2016;16:22.
78. Spielberger CD, Gorsuch, R. L., Lushene, R., Vagg, P. R., & Jacobs, G. A. . Manual for the State-Trait Anxiety Inventory. Consulting Psychologists Press. 1983.
79. Baker Frank DM, Zabora, James, Polland Adrienne, Dudley William. A POMS short form for cancer patients: Psychometric and structural evaluation. Psycho-oncology. 2002;11.
80. Dyk KV, Crespi CM, Petersen L, Ganz PA. Identifying Cancer-Related Cognitive Impairment Using the FACT-Cog Perceived Cognitive Impairment. JNCI Cancer Spectrum. 2019;4(1).
81. Wang JY, Abdi H, Bakhadirov K, Diaz-Arrastia R, Devous MD, Sr. A comprehensive reliability assessment of quantitative diffusion tensor tractography. Neuroimage. 2012;60(2):1127-38.
82. Jenkinson M, Bannister P, Brady M, Smith S. Improved optimization for the robust and accurate linear registration and motion correction of brain images. Neuroimage. 2002;17(2):825-41.
83. Desikan RS, Segonne F, Fischl B, Quinn BT, Dickerson BC, Blacker D, et al. An automated labeling system for subdividing the human cerebral cortex on MRI scans into gyral based regions of interest. Neuroimage. 2006;31(3):968-80.
84. McMahon SJ. The linear quadratic model: usage, interpretation and challenges. Phys Med Biol. 2018;64(1):01TR.
85. van Leeuwen CM, Oei AL, Crezee J, Bel A, Franken NAP, Stalpers LJA, et al. The alfa and beta of tumours: a review of parameters of the linear-quadratic model, derived from clinical radiotherapy studies. Radiat Oncol. 2018;13(1):96.
86. Law MY, Liu B. Informatics in radiology: DICOM-RT and its utilization in radiation therapy. Radiographics. 2009;29(3):655-67.
87. Iglesias JE, Insausti R, Lerma-Usabiaga G, Bocchetta M, Van Leemput K, Greve DN, et al. A probabilistic atlas of the human thalamic nuclei combining ex vivo MRI and histology. Neuroimage. 2018;183:314-26.
88. Woolrich MW, Jbabdi S, Patenaude B, Chappell M, Makni S, Behrens T, et al. Bayesian analysis of neuroimaging data in FSL. Neuroimage. 2009;45(1 Suppl):S173-86.
89. Smith SM, Jenkinson M, Woolrich MW, Beckmann CF, Behrens TE, Johansen-Berg H, et al. Advances in functional and structural MR image analysis and implementation as FSL. Neuroimage. 2004;23 Suppl 1:S208-19.

90. Jenkinson M, Beckmann CF, Behrens TE, Woolrich MW, Smith SM. Fsl. Neuroimage. 2012;62(2):782-90.
91. Smith SM. Fast robust automated brain extraction. Hum Brain Mapp. 2002;17(3):143-55.
92. Andersson JLR, Sotiropoulos SN. An integrated approach to correction for off-resonance effects and subject movement in diffusion MR imaging. Neuroimage. 2016;125:1063-78.
93. Basser PJ, Mattiello J, LeBihan D. Estimation of the effective self-diffusion tensor from the NMR spin echo. J Magn Reson B. 1994;103(3):247-54.
94. Hua K, Zhang J, Wakana S, Jiang H, Li X, Reich DS, et al. Tract probability maps in stereotaxic spaces: analyses of white matter anatomy and tract-specific quantification. Neuroimage. 2008;39(1):336-47.
95. Woolrich MW, Ripley BD, Brady M, Smith SM. Temporal autocorrelation in univariate linear modeling of FMRI data. Neuroimage. 2001;14(6):1370-86.
96. Evans AC, Janke AL, Collins DL, Baillet S. Brain templates and atlases. Neuroimage. 2012;62(2):911-22.
97. Kim JW, Andersson JL, Seifert AC, Sun P, Song SK, Dula C, et al. Incorporating non-linear alignment and multi-compartmental modeling for improved human optic nerve diffusion imaging. Neuroimage. 2019;196:102-13.
98. Salimi-Khorshidi G, Douaud G, Beckmann CF, Glasser MF, Griffanti L, Smith SM. Automatic denoising of functional MRI data: combining independent component analysis and hierarchical fusion of classifiers. Neuroimage. 2014;90:449-68.
99. Griffanti L, Salimi-Khorshidi G, Beckmann CF, Auerbach EJ, Douaud G, Sexton CE, et al. ICA-based artefact removal and accelerated fMRI acquisition for improved resting state network imaging. Neuroimage. 2014;95:232-47.
100. Sporns O. The human connectome: a complex network. Ann N Y Acad Sci. 2011;1224:109-25.
101. Sporns O. Structure and function of complex brain networks. Dialogues Clin Neurosci. 2013;15(3):247-62.
102. Rubinov M, Sporns O. Complex network measures of brain connectivity: uses and interpretations. Neuroimage. 2010;52(3):1059-69.
103. Benjamini Y, Hochberg Y. Controlling the False Discovery Rate: A Practical and Powerful Approach to Multiple Testing. Journal of the Royal Statistical Society: Series B (Methodological). 1995;57(1):289-300.
104. Cho B. Intensity-modulated radiation therapy: a review with a physics perspective. Radiat Oncol J. 2018;36(1):1-10.
105. Farahani FV, Karwowski W, Lighthall NR. Application of Graph Theory for Identifying Connectivity Patterns in Human Brain Networks: A Systematic Review. Front Neurosci. 2019;13:585.

**Figure 1.** Study schema

**Figure 2.** MRI Data Processing Pipeline. FC: Functional Connectivity; FA: Fractional Anisotropy; MD: Mean Diffusivity; AD: Axial Diffusivity; RD: Radial Diffusivity; DTI: Diffusion Tensor Imaging; SC: Structural Connectivity; GTV: Gross Target Volume; CT: Computed Tomography; RT: Radiotherapy; dMRI: Diffusion MRI; rs-fMRI: resting state functional MRI; FEAT: FMRI Expert Analysis Tool; MELODIC: Multivariate Exploratory Linear Optimized Decomposition into Independent Components; FIX: FMRIB's ICA-based Xnoisefier.

**Figure 3.** Representative Images from subject with vestibular schwannoma. (A) RT dose map from RT structure set, mapped to CT image, and scaled. (B) T1w structural image co-registered with CT image and RT dose map via affine transformation (yellow circle shows acoustic schwannoma). (C) T1w image with gross target volume (GTV, yellow circle) used to mask tumor prior to processing. (D) Subcortical and cortical structures obtained from brain parcellation, with vestibular schwannoma excluded (yellow arrow).

**Figure 4.** Representative functional connectivity correlation matrices. Matrices are computed using the Pearson correlation coefficient between every time course for all pairs of nodes. Matrices are thresholded at 0.5 and normalized. The average of all subject specific correlation matrices at baseline (A) and 6-months post RT (B). The color bar represents the normalized correlation coefficient between pairs of nodes.

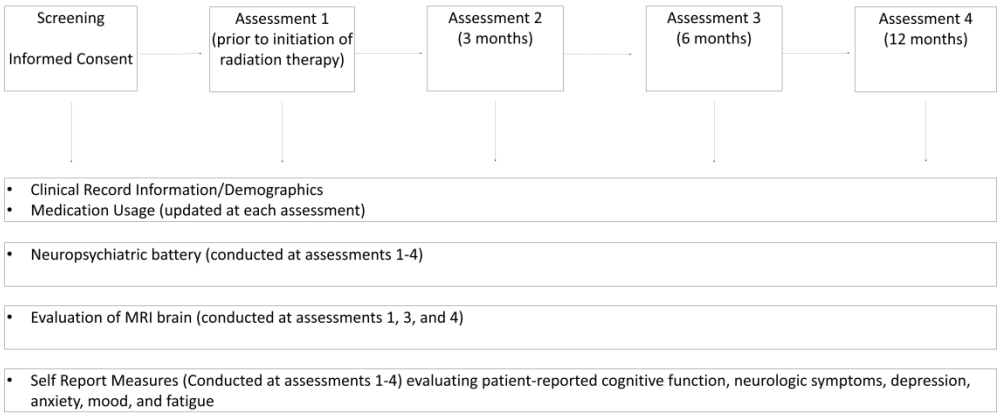


Study schema

1387x581mm (150 x 150 DPI)

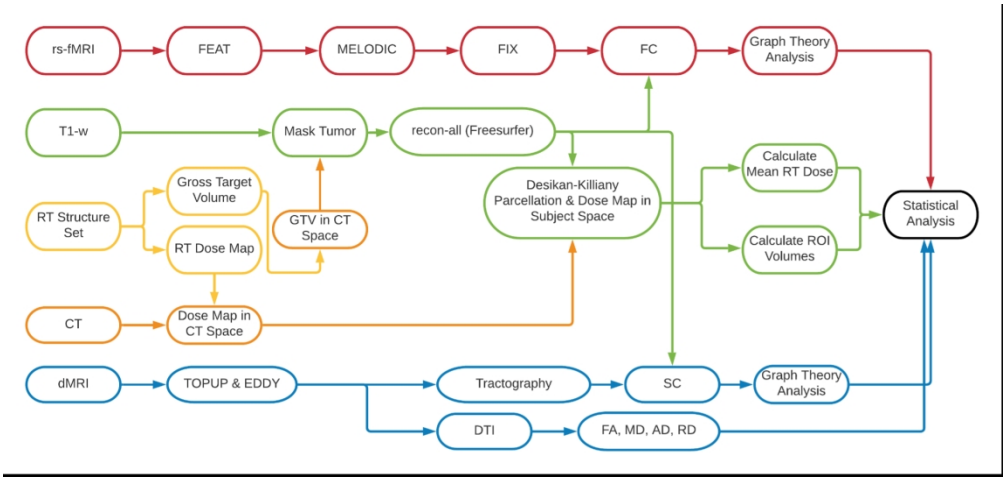


MRI Data Processing Pipeline. FC: Functional Connectivity; FA: Fractional Anisotropy; MD: Mean Diffusivity; AD: Axial Diffusivity; RD: Radial Diffusivity; DTI: Diffusion Tensor Imaging; SC: Structural Connectivity; GTV: Gross Target Volume; CT: Computed Tomography; RT: Radiotherapy; dMRI: Diffusion MRI; rs-fMRI: resting state functional MRI; FEAT: FMRI Expert Analysis Tool; MELODIC: Multivariate Exploratory Linear Optimized Decomposition into Independent Components; FIX: FMRIB's ICA-based Xnoisefier.

103x49mm (500 x 500 DPI)

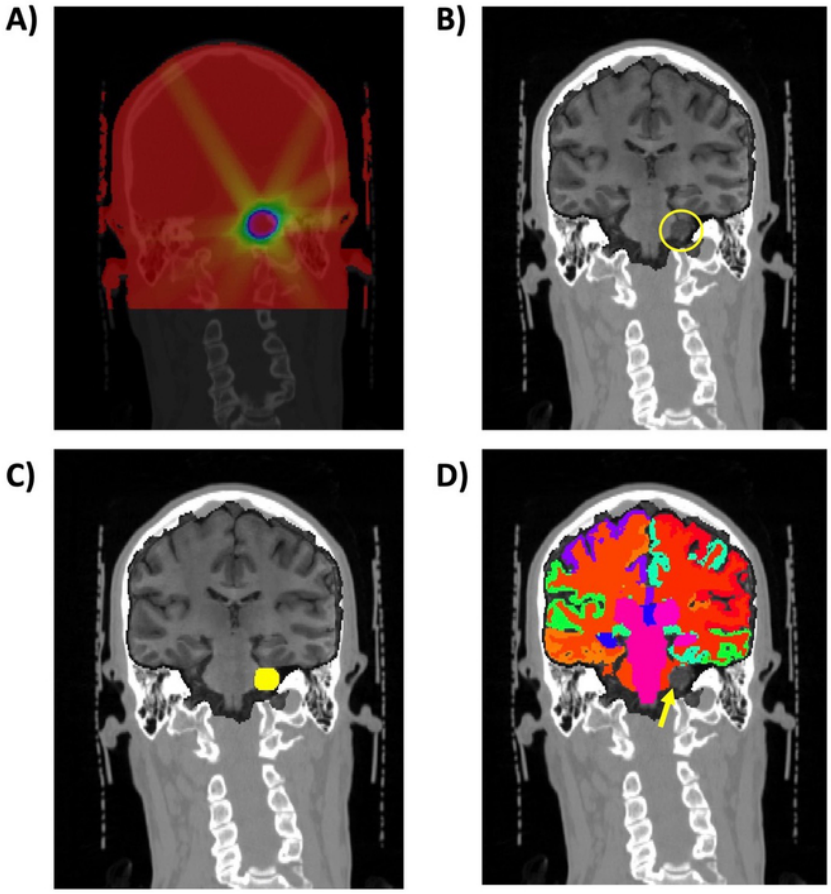


Representative Images from subject with vestibular schwannoma. (A) RT dose map from RT structure set, mapped to CT image, and scaled. (B) T1w structural image co-registered with CT image and RT dose map via affine transformation (yellow circle shows acoustic schwannoma). (C) T1w image with gross target volume (GTV, yellow circle) used to mask tumor prior to processing. (D) Subcortical and cortical structures obtained from brain parcellation, with vestibular schwannoma excluded (yellow arrow).

67x64mm (300 x 300 DPI)

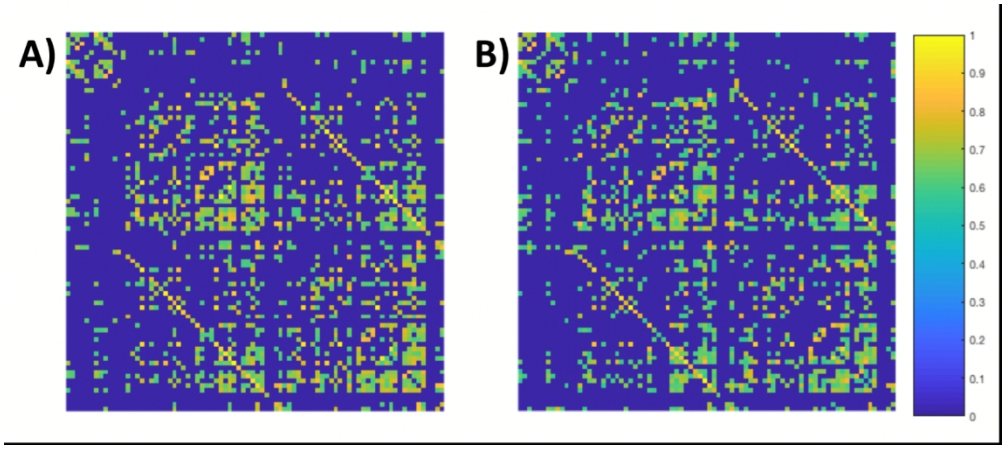


Representative functional connectivity correlation matrices. Matrices are computed using the Pearson correlation coefficient between every time course for all pairs of nodes. Matrices are thresholded at 0.5 and normalized. The average of all subject specific correlation matrices at baseline (A) and 6-months post RT (B). The color bar represents the normalized correlation coefficient between pairs of nodes.

88x38mm (500 x 500 DPI)

BMJ Open

# Cognitive and neuroimaging outcomes in individuals with benign and low-grade brain tumors receiving radiotherapy: a protocol for a prospective cohort study



| | |
|---|---|
| Journal: | *BMJ Open* |
| Manuscript ID | bmjopen-2022-066458.R1 |
| Article Type: | Protocol |
| Date Submitted by the Author: | 07-Jan-2023 |
| Complete List of Authors: | Hardy, Sara; University of Rochester Medical Center, Department of Radiation Oncology; University of Rochester Medical Center, Department of Neurology<br>Finkelstein, Alan J.; University of Rochester, Department of Biomedical Engineering; University of Rochester Medical Center<br>Tivarus, Madalina; University of Rochester Medical Center; University of Rochester Medical Center, Department of Imaging Sciences<br>Culakova, Eva; University of Rochester Medical Center, Department of Surgery<br>Mohile, Nimish; University of Rochester Medical Center, Department of Neurology<br>Weber, Miriam; University of Rochester Medical Center, Department of Neurology; University of Rochester Medical Center, Department of Obstetrics and Gynecology<br>Lin, Edward; University of Rochester Medical Center, Department of Imaging Sciences<br>Zhong, Jianhui; University of Rochester, Department of Biomedical Engineering; University of Rochester Medical Center<br>Usuki, Kenneth; University of Rochester Medical Center, Department of Radiation Oncology<br>Schifitto, Giovanni; University of Rochester Medical Center, Department of Neurology, Department of Imaging Sciences<br>Milano, Michael; University of Rochester Medical Center, Department of Radiation Oncology<br>Janelsins-Benton, MC; University of Rochester Medical Center, Department of Radiation Oncology; University of Rochester Medical Center, Department of Surgery |
| Primary Subject Heading: | Radiology and imaging |
| Secondary Subject Heading: | Neurology, Oncology |
| Keywords: | RADIOTHERAPY, Neurological oncology < NEUROLOGY, Magnetic resonance imaging < RADIOLOGY & IMAGING, Radiation oncology < RADIOTHERAPY |
| | |

# Cognitive and neuroimaging outcomes in individuals with benign and low-grade brain tumors receiving radiotherapy: a protocol for a prospective cohort study

**Sara J Hardy[1,2,‡], Alan J. Finkelstein[3,4,‡], Madalina Tivarus[4,5], Eva Culakova[7], Nimish Mohile[2], Miriam Weber[2,6], Edward Lin[5], Jianhui Zhong[3,4,5,9], Kenneth Usuki[1], Giovanni Schifitto[2,5,8], Michael T Milano[1], Michelle C. Janelsins[1,7]**

**‡Authors contributed equally to the manuscript**

**Affiliations:**

[1]Department of Radiation Oncology, University of Rochester Medical Center, Rochester, NY, USA
[2]Department of Neurology, University of Rochester Medical Center, Rochester, NY, USA
[3]Department of Biomedical Engineering, University of Rochester, Rochester, NY, USA
[4]Center for Advanced Brain Imaging and Neurophysiology, University of Rochester Medical Center, Rochester, NY, USA
[5]Department of Imaging Sciences, University of Rochester Medical Center, Rochester, NY, USA
[6]Department of Obstetrics and Gynecology, University of Rochester Medical Center, Rochester, NY, USA
[7]Department of Surgery, University of Rochester Medical Center, Rochester, NY, USA
[8]Department of Electrical and Computer Engineering, University of Rochester, Rochester, NY, USA
[9]Department of Physics and Astronomy, University of Rochester, Rochester, NY, USA

**Corresponding author:**

**Sara J Hardy[1,2]**
sara_hardy@urmc.rochester.edu
[1]Department of Radiation Oncology, University of Rochester Medical Center, Rochester, NY, USA
[2]Department of Neurology, University of Rochester Medical Center, Rochester, NY, USA

**Keywords: neurological oncology, radiotherapy, magnetic resonance imaging, radiation oncology**

## ABSTRACT

**Introduction:** Radiation-induced cognitive decline (RICD) occurs in 50-90% of adult patients 6 months post-treatment. In patients with low grade and benign tumors with long expected survival, this is of paramount importance. Despite advances in radiation (RT) treatment delivery, better understanding of structures important for RICD is necessary to improve cognitive outcomes. We hypothesize that RT may affect network topology and microstructural integrity on MRI prior to any gross anatomical or apparent cognitive changes. In this longitudinal cohort study, we aim to determine the effects of RT on brain structural and functional integrity and cognition.

**Methods and Analysis:** This study (ClinicalTrials.gov NCT04390906) will enroll patients with benign and low-grade brain tumors receiving partial brain radiotherapy. Patients will receive either hypofractionated (>2 Gy/fraction) or conventionally fractionated (1.8-2 Gy/fraction) RT. All participants will be followed for 12 months, with MRIs conducted pre-RT and 6- and 12-months post-RT, along with a battery of neurocognitive tests and questionnaires. The study was initiated in late 2018 and will continue enrolling through 2024 with final follow ups completing in 2025. The neurocognitive battery assesses visual and verbal memory, attention, executive function, processing speed, and emotional cognition. MRI imaging protocols incorporate diffusion tensor imaging (DTI) and resting state fMRI (rs-fMRI) to assess structural connectivity (SC) and functional connectivity (FC), respectively. We will estimate the association between radiation dose, imaging metrics, and cognitive outcomes.

**Ethics and Dissemination:** This study has been approved by the Research Subjects Review Board at the University of Rochester (STUDY00001512: Cognitive changes in patients receiving partial brain radiation). All results will be published in peer-reviewed journals and at scientific conferences.


## STRENGTHS AND LIMITATIONS OF THIS STUDY

- Strengths:
  - Limiting the study to participants with only benign and low-grade brain tumors helps mitigate confounding factors such as variation in tumor biology and normal tissue infiltration..
  - Prospective design with baseline evaluation prior to radiation allows capture of longitudinal changes in imaging and cognitive outcomes.
  - Use of open-source software assures transparency, reproducibility, and implementation of the proposed protocol by other investigators.
  - Inclusion of patients receiving hypofractionated radiation, which has increasingly been utilized in benign and low grade brain tumors, is highly important since much of the data focuses on conventionally fractionated radiation.
- Limitations:
  - Heterogeneity of patient population including tumor type, size, and location, radiation techniques, patient clinical factors including age, other cancer treatments including chemotherapy and surgery is a significant limitation; however, these factors will be adjusted for in analysis and improve generalizability of results.

## INTRODUCTION

**Rationale and Evidence Gaps:** Cognitive impairment in patients with brain tumors has a major impact on quality of life and on the ability to function at work and in daily life (1-4). Deficits manifest clinically as impairments in multiple cognitive domains including memory, attention, and executive function (5, 6). The etiology is often multifactorial; contributing factors may include anxiety and/or depression, tumor location and pathology, comorbidities, and age, as well as effects from treatment (chemotherapy, surgery, and/or radiation therapy(7)). Notably, RICD is observed in more than 30% of patients at 4 months after partial or whole brain RT and in more than 50% at 6 months (8). RICD is particularly important in patients with low grade and benign tumors who are expected to have long-term survivals. In these patients, treatment selection to maximize quality of life and minimize cognitive deficits is imperative. Considerable efforts have been directed toward understanding and preventing radiation-induced cognitive decline (RICD), an important late effect of radiation therapy (5, 9, 10). To date, multiple mechanisms underlying RICD have been elucidated, including damage to sites of neurogenesis (11, 12), neuroinflammation (13, 14), neuronal dysfunction (15), and vascular changes (16-18).

RICD can occur in the absence of any gross anatomical changes. Advanced magnetic resonance imaging (MRI) techniques, however, may be able to detect effects from RT early on and may help elucidate mechanisms of radiation damage in RICD (19). MRI can examine volumetric and connectivity changes (both functional and structural) as well as changes in brain vasculature and perfusion. MRI may ultimately provide tools to identify patients at risk for RICD and help to direct efforts to prevent or ameliorate cognitive decline. Accordingly, accurate modeling of neurocognitive function with neuropsychological tests and correlation with *in vivo* imaging findings may help to identify putative biomarkers for routine quantitative evaluation of cognitive changes in patients with RICD. Novel MRI biomarkers of RICD are essential to improve understanding of how RT affects the brain structurally and functionally, to identify potential targets and therapeutics to mitigate RICD, and to improve initial RT plans to decrease complication rates.

RT affects both gray and white matter structures, yet the functional implications of these changes are actively being investigated. Studies have shown that cranial RT is associated with dose-dependent atrophy of the cortex (20), hippocampus (21) and amygdala (22) on T1-weighted (T1w) MRI. The hippocampus in particular has garnered attention as a vulnerable structure in the setting of RT; where RT has been shown to reduce neurogenesis (23, 24) and the pool of neural stem cells in the dentate gyrus (25, 26). Additionally, radiation dose to the hippocampus has also been shown to predict Hopkins Verbal Learning Test scores after brain irradiation (27). **Currently, the hippocampus is the only intracranial structure for which validated dose constraints are used in standard treatment planning (28-31).** NRG Oncology CC001 showed that conformal avoidance of the bilateral hippocampi (important structures in learning and memory) during whole brain RT reduced the risk of cognitive decline at 6 months from 68.2% to 59.5% (32). Despite advances in understanding of the role of the hippocampus in RICD, however, nearly 60% of patients still experience diminished cognitive function after RT despite conformal avoidance of the hippocampus. Moreover, recent studies have shown that radiation dose to the corpus callosum and surrounding white matter tracts can impact attention and processing speed at 6 months post-RT (33), executive function with radiation damage to the anterior cingulate cortex (34), damage to perisylvian white matter can predict language dysfunction (35), and damage to the hippocampus, temporal pole, and entorhinal cortex can predict changes in visuospatial memory (36). Thus, while the hippocampus is undoubtedly an important structure in memory formation, the singular focus on this region likely belies the complexity of structures and networks involved in memory formation and ignores the contribution of other anatomic structures to cognitive deficits seen post-therapy.

**Novelty and Innovation:** While there have been some strides made in understanding RICD, there remain significant gaps in our knowledge, which our study hopes to address. These include applications of rs-fMRI in prediction of RICD, evaluation of cognitive outcomes after hypofractionated radiation for low grade and benign brain tumors, evaluation of novel areas of interest that could contribute to cognitive decline, and integration of established autosegmentation software such as Freesurfer with radiation dose information.

Whole brain networks can be evaluated by analyzing structural and functional connections within the brain and their connections to function and behavior (37). Structural connectivity in the brain is measured by tracing white matter tracts derived from diffusion tensor imaging (DTI), (38). DTI evaluates the direction and magnitude of water molecular diffusion in a three-dimensional space (diffusion tensor) and can provide information on anisotropic diffusion. Additional quantitative metrics such as the fractional anisotropy (FA), axial diffusivity (AD), mean diffusivity (MD), and radial diffusivity (RD) can be obtained from DTI and can help describe different disease states such as demyelination (39, 40). Studies using DTI have shown that RT results in atrophy, demyelination of white matter, and gliosis (41) particularly in patients with a history of demyelinating diseases (42). Partial brain RT has also been shown to result in decreased AD and increased RD within the parahippocampal cingulum, where these changes are correlated with declines in verbal memory and fluency (43). Notably, reconstruction of fiber tracts in brain tumors and surrounding tissues is confounded by false continuities within the tumor and surrounding edema (44). Accordingly, advanced diffusion methods have recently been developed to model and eliminate free water with single-shell diffusion weighted imaging data, to more accurately model the tissue microstructure of surrounding normal brain tissue (45). However, similar to gross volumetric changes, apparent evidence of white matter atrophy and demyelination may not be discernable prior to 6 months or 1-year post-RT (46, 47). Resting state functional MRI (rs-fMRI) can be used to evaluate functional connectivity. In particular, graph-theory analysis of functional connectivity has revealed topological organization of brain networks (48), which has been used to investigate how network topology is affected in development (49), aging (50) and pathology (51-53). Graph theory-based approaches treat the brain as a network of nodes and edges, where nodes can be a region of interest (ROI) or a single voxel. Edges are the connections between each node. These graphical relationships can then be modeled as a correlation matrix, in which cross correlation is performed to determine the strength between pairs of nodes. Analysis of these matrices has revealed the brain to be highly modular (54, 55), with specific network hubs (areas of many connections to other nodes)(56), which have been shown to change in the setting of pathology and RT (57). Nevertheless, it is not known whether functional network changes can predict RICD or precede structural changes on MRI.

There has been limited evaluation of whether rs-fMRI can be used to predict early radiation changes. This may be partially due to difficulty in using rs-fMRI in high grade glioma (33). Other studies have consistently demonstrated that IDH wild type gliomas (ie. gliomas with more aggressive histology) have greater impact on functional connectivity metrics such as global functional connectivity derived from rs-fMRI (58) as well as impact baseline cognitive status to a greater degree prior to any treatment (59). When limited to select patients, this modality may be useful as an MRI biomarker in early grade and benign brain tumor patients receiving radiation. Further studies focused on that population and excluding high grade glioma patients, such as this one, are needed. Whole brain metrics such as functional connectivity may provide early identification of participants who are at risk of decline and can be targeted with novel therapeutics, either by using advanced RT techniques to improve RT plans or use of radioprotective pharmaceuticals. Preliminary studies are limited but suggest that rs-fMRI and functional connectivity represent a promising modality with which to develop dose constraints and mitigate cognitive decline after RT (60-62).

**Study Aims:** Investigation into structures outside the hippocampus that can be spared in order to improve cognitive outcomes remains an area of active study. We have the most data for RICD related to radiation dose to the corpus callosum (33, 63) and hippocampus (31, 32). However, we currently have no valid dose constraints for the structures outside the hippocampus including the corpus callosum. Development of dose constraints and investigation of which structures can be avoided and lead to improvement in clinical outcomes is an area of active research as we seek to understand the complex structural and functional relationships that lead to RICD (64).

Additionally, radiosurgery and fractionated radiosurgery are important modalities used frequently in the treatment of benign brain tumors. With the increased use of hypofractionation and radiosurgery, it is important to establish dose constraints that are valid in the setting of high dose per fraction (65). As of now, we have little data on dose constraints for cognitive avoidance structures in the setting of hypofractionation, and much is extrapolated from studies of conventional fractionation.

Accordingly, this study will evaluate the effects of RT in patients with benign and low-grade brain tumors using multimodal neuroimaging and a battery of neurocognitive tests. We hypothesize that radiation induced damage will manifest prior to gross anatomical changes via alterations in network topology and microstructural integrity. Ultimately, we aim to establish structures beyond the hippocampus that are vulnerable to RT and develop dose constraints to minimize the risk and progression of RICD in this vulnerable patient population.

## METHODS and ANALYSIS

### Study Design

A total of 75 patients with benign and low-grade brain tumors planned to receive partial brain RT, either hypofractionated (>2 Gy/fraction) or conventionally fractionated (1.8-2 Gy/fraction), will be enrolled at the Wilmot Cancer Institute. All participants provide written informed consent according to the Institutional Review Board (IRB) approved protocol prior to any evaluation. Participants are followed for 12 months.

Key inclusion criteria include 1) age ≥18-years; 2) patients with benign or low-grade brain tumors including grade 2 IDH-mutant astrocytoma, grade 2 oligodendroglioma, grade 1 and 2 meningiomas, vestibular schwannomas, pituitary adenomas, craniopharyngiomas, hemangiopericytomas, or other benign or low-grade brain tumors; 3) planned to receive either conventional or hypofractionated RT; 4) no contraindication to gadolinium-enhanced MRI. Surgical excision and/or chemotherapy prior to enrollment is permitted.

Key exclusion criteria include 1) Prior cranial RT; 2) Inability to participate in neurocognitive testing; 3) Intractable seizures; 4) Non-English speaking; 5) Aphasia limiting ability to participate in neurocognitive testing.

Participants will undergo three comprehensive evaluations (baseline, 6-month, and 12-month time points) that include clinical evaluation, MRI, a battery of neurocognitive tests, and questionnaires which evaluate patient-reported cognition, fatigue, anxiety, and depression. An additional 3-month timepoint includes questionnaires and neurocognitive testing only (Figure 1).

### Patient and Public Involvement

Patients will be involved in the design and conduct of this research as follows: After completion of this study, we will plan to further tailor the study design for a larger study by conducting interviews with participants. Once the results have been published, participants will be informed via email.

**Neurocognitive Testing**

Assessments of neurocognitive and functional performance are performed to evaluate neurocognitive changes post-RT. The components of the neurocognitive testing battery are described in Table 1. The battery includes the standard tests recommended by the International Cognition and Cancer Task Force (66) testing verbal memory (HVLT-R, (67, 68), verbal fluency (COWA, (69), and executive function (TMT(70, 71). However, the battery additionally includes the BVMT-R, which has a similar format to the HVLT-R but focuses on visuospatial learning and memory (36), as well as additional iPad-based tests from Cambridge Cognition which have been shown to be valid and sensitive in the assessment of cancer-related cognitive impairment (72-74). Neuropsychological testing is administered by trained study coordinators using a standardized testing manual; study coordinators are supervised by the study team with expertise in neurology, neuropsychology and cognitive science. Raw scores will be used in analysis and adjusted for covariates such as age. Testing is performed in a quiet, comfortable room without distractions.

**Table 1.** Description and platform of tests in cognitive battery

| Test | Description | Cognitive Domain | Platform |
|---|---|---|---|
| **Wide Range Achievement Test-4 (WRAT-4)** | Word reading | Cognitive reserve, education level | Paper-based |
| **Hopkins Verbal Learning Test-Revised (HVLT-R)** | Immediate and delayed recall of a word list | Verbal learning and memory | Paper-based |
| **Controlled Oral Word Associated Test (COWA)** | Number of words the participant can provide in a category over one minute | Verbal fluency | Paper-based |
| **Trail Making Test A and B (TMT-A and TMT-B)** | Connect circles containing a series of numbers (A) or numbers and letters (B) in a pattern | Executive function | Paper-based |
| **Brief Visuospatial Memory Test-Revised (BVMT-R)** | Immediate and delayed recall of a series of shapes and designs | Visuospatial learning and memory | Paper-based |
| **Emotional Recognition Task (ERT)** | Identification of the emotion indicated by a facial expression | Emotional and social cognition | Cambridge cognition |
| **Spatial Working Memory (SWM)** | Use of strategy to find a yellow token behind colored boxes | Executive function, visuospatial working memory | Cambridge cognition |
| **Paired Associates Learning (PAL)** | Match the pattern to the box where it was previously displayed | Visuospatial episodic memory and new learning | Cambridge cognition |
| **Delayed Matching to Sample (DMS)** | Matching of complex visual patterns | Visual matching ability and short-term visual recognition memory | Cambridge cognition |
| **Reaction Time Task (RTT)** | Select a circle in which a yellow dot appears | Assessment of motor and mental response speed | Cambridge cognition |

**Patient Reported Outcomes**

Patient reported outcome measures of symptoms that may influence cognition are recorded longitudinally so that they can be studied and accounted for in analyses. These symptoms include fatigue, anxiety, and depression using validated measures including the Functional Assessment of Cancer Therapy-Brain (FACT-Br, neurologic symptoms in brain tumor patients, (75), Functional Assessment of Cancer-Fatigue (FACIT-Fatigue, symptoms of fatigue, (76), Patient Health Questionnaire-9 (PHQ-9, symptoms of depression, (77), State-Trait Anxiety Inventory (STAI, (78), and Short Form of the Profile of Mood States-2 (POMS2-SF, subscales of anger-hostility, confusion-bewilderment, depression-dejection, fatigue-inertia, tension-anxiety, vigor-activity, and friendliness, (79). Subjective cognition is measured using the Functional Assessment of Cancer Therapy-Cognition (FACT-Cog, (80) for comparison with scores on objective neurocognitive testing.

**Demographic and Clinical Information**

Patient characteristics that may affect cognitive outcomes and trajectories are recorded, including age, education level, comorbidities including diabetes, hypertension, autoimmune disease, tumor hemisphere, tumor site, tumor pathology, prior surgeries, employment status, smoking status, alcohol use, sex/gender, hypopituitarism, menopausal status, steroid use, use of medications that can affect cognition and mood, and exposure to chemotherapy.

**Radiotherapy Planning**

Each patient is planned and treated per standard of care by their treating radiation oncologist. RT plans for single fraction or fractionated radiosurgery are created using BrainLAB Elements® planning software. All other plans were created using Varian Eclipse® treatment planning software. For consistency, all radiation dose maps were calculated in Eclipse for all patients using a 1 mm x 1 mm grid.

**MRI Acquisition**

All imaging is performed on a 3T GE Discovery 750 MRI system (Milwaukee, WI, USA), equipped with an 8-channel head coil. High-resolution T1w anatomical images are acquired using a 3D BRAVO FSPGR sequence with the following parameters: repetition time (TR)= 8.2 ms, echo time (TE)= 3.2 ms, field of view (FOV) 256 $mm^2$, resolution 1x1x1$mm^3$.

Blood oxygen level dependent (BOLD) rs-fMRI is acquired using a BOLD sensitive gradient-echo echo planar imaging (GE-EPI) sequence with the following parameters: TR=2000ms, TE=30ms, FOV=192$mm^2$, resolution 3x3x3 $mm^3$, 150 volumes.

In order to evaluate white matter integrity and microstructural changes, we make use of a standard clinical DTI protocol with 30 diffusion directions, demonstrated to be sufficient for reconstructing white matter fiber tracts and not to affect test-retest reliability (81). DTI is acquired using a 2D axial single-shot dual spin-echo EPI (SE-EPI) sequence with the following parameters: TR= 10,000ms, TE= 81ms, FOV=256$mm^2$, resolution 2x2x2 $mm^3$, 30 diffusion weighted directions with b=1000s/$mm^2$ and 4 b=0 reference images.

**MRI Data Processing**

Herein we describe a comprehensive image analysis pipeline, which includes preprocessing, data cleaning, and post-processing for each imaging modality, including advanced modelling and calculation of quantitative imaging biomarkers (Figure 2).

All image processing is completed within URMC servers in the Center for Integrated Research Computing (CIRC), using BHWARD, a HIPAA compliant server.

**RT Dose Calculations**

The RT dose map is first scaled and mapped with CT images using pydicom (version 1.4). T1w images are registered to patient-specific CT space using FMRIB's Linear Image Registration Tool (FLIRT, (82). Patient-specific parcellations derived from the Desikan-Killiany (83) atlas using Freesurfer are registered with the RT dose map. The mean, maximum, and minimum RT doses are extracted from each ROI, and the 2 Gy/fraction equivalent dose (EQD2) is calculated using the linear quadratic model (84), with an $\alpha/\beta$ equal to 3, to model the radiosensitivity of normal brain tissue (85).

**T1w**

T1w images are processed by first masking out the tumor using the gross target volume (GTV) as contoured by the primary radiation oncologist from the RT structure set (86), delineated on planar MRI and CT imaging, using nibabel (https://nipy.org, version 3.1.1). This is achieved by mapping the GTV to the CT images in patient space, and then performing an affine transform to register the T1-w images to the patient specific CT images (Figure 3). Thereafter, segmentation is performed using the tumor masked T1-w in Freesurfer (version 6.0.0, http://surfer.nmr.harvard.edu). The Freesurfer pipeline is run independently for each participant at each time point (pre-RT, 6-months, and 12-months post-RT). Briefly, processing includes skull-stripping and removal of non-brain tissue, motion correction, intensity normalization, automated Talairach transformation, white matter segmentation, and cortical parcellation using the Desikan-Killiany atlas (83), which includes cortical and subcortical regions of interest (ROIs). Subsequent segmentation of thalamic nuclei are also performed using a probabilistic atlas based on ex vivo MRI and histology (87). ROIs will include whole brain gray and white matter, cerebral hemispheres and subcortical gray matter (hippocampus, amygdala, caudate, putamen, thalamus, nucleus basalis of Meynert), as well as white matter tracts including cingulum, fornix, parahippocampal white matter, and corpus callosum.

**Diffusion Imaging**

DTI data is pre-processed using FMRIB's Software Library (FSL, (88-91) diffusion toolbox (FDT, http://fsl.fmrib.ox.ac.uk/fsl). Briefly, inter-volume patient motion, brain extraction using BET (91), and eddy-current induced distortion correction are performed using EDDY (92). The diffusion tensors are then fit on eddy-corrected data using DTIFIT (93). DTIFIT fits a diffusion tensor model at each voxel and provides the 3 principal eigenvectors and eigenvalues of the diffusion tensor, from which the fractional anisotropy (FA), mean diffusivity (MD), axial diffusivity (AD), and radial diffusivity (RD) can be measured (93). All images are then registered to MNI standard space and interpolated to 1 $mm^3$ voxels. Binary gross target volume masks are then used to mask out abnormal tissue in processed maps. The JHU white-matter tractography atlas, composed of 20 structures identified using probabilistic tractography, is then used to extract mean FA, MD, AD, and RD values from regions of interest (94).

**Functional Imaging**

rs-fMRI data is processed using FSL's FMRI Expert Analysis Tool (FEAT, version 6.00)(95). Registration to high resolution structural space is carried out using a two-stage registration. First rs-fMRI data is registered to high-resolution structural space using FMRIB's Linear Image Registration Tool (FLIRT, (82), and then registration to MNI standard space (96) is further refined using FMRIB's Nonlinear Image Registration Tool (FNIRT, (97). Since field maps were not acquired as part of the clinical scan protocol, a 12 degrees-of-freedom affine transformation was used for linear and nonlinear registration. All registrations are visually inspected during processing. Further preprocessing includes

skull stripping using BET (91), motion correction using MCFLIRT (82), slice-time correction, spatial smoothing using a Gaussian kernel of FWHM 5mm, and high-pass temporal filtering.

Single-session independent component analysis (ICA) is then performed for each participant using probabilistic ICA implemented in FSL's Multivariate Exploratory Linear Optimized Decomposition into Independent Components (MELODIC, Version 3.15). MELODIC de-composes input data into separate time courses and spatial maps using probabilistic principal component analysis (PCA). FMRIB's ICA-based Xnoisifier (FIX, (98, 99) is then used to further denoise functional data by automatically classifying signal versus noise components from the time series data. FIX is run using the standard pre-trained data (TR=3s, 3.5x3.5x3.5mm resolution, 6 minutes) which was preprocessed using default FEAT processing. All images and components are visually inspected for accuracy prior to further processing.

Once all fMRI data has been preprocessed, the denoised functional data is used to construct participant specific functional connectivity (FC) matrices. Participant specific atlases generated using Freesurfer are then registered to the MNI standard space and used to extract the mean time series from each ROI. This is done to ensure that only functional regions outside of the tumor are used to construct FC matrices. FC matrices are then generated by computing the cross correlation between all pairs of nodes (ROIs), using the Pearson correlation coefficient (Figure 4).

Participant specific FC matrices are then analyzed using the Brain Connectivity Toolbox (100) in MATLAB (R2020a). Participant specific correlation matrices are thresholded to yield weighted undirected networks, and analyzed using graph theory to yield measures of functional integration and segregation. Global measures of integration, including global efficiency, transitivity and modularity, are then computed for further statistical analysis (101). Local measures of segregation, including clustering coefficient and local efficiency (Table 2), are also computed for each ROI for further statistical analysis. A more thorough review of graph theory-based measures for rs-fMRI may be found in Rubinov and Sporns, 2010 (102).

**Table 2.** Overview of graph theory measures used to analysis resting state functional connectivity and structural connectivity obtained from diffusion tractography. A more in depth review of graph theory and graph theory measures can be found in Rubinov and Sporns, 2010 (93)

| Measurement | Definition | Equation |
|---|---|---|
| **Node Degree** | The number of connections between one node and the rest of the network | $k_i = \Sigma(a_{ij})$ |
| **Clustering Coefficient** | The number of connections between the neighbors of a node. | $2t/(k(k-1);$ k is the node degree; t is the fraction of triangles around a node. |
| **Efficiency** | Inverse of path length (minimum number of edges to traverse from one node to another) | $\frac{1}{N(N-1)}\Sigma\left(\frac{1}{d_{ij}}\right)$ Where $d_{ij}$ is the shortest path length between nodes i and j |
| **Modularity** | Areas of highly interconnected nodes, with few connections to nodes in other modules. | $Q = \frac{1}{l}\Sigma\left(a_{ij} - \frac{(k_i k_j)}{l}\right)\delta(m_i,m_j)$ |

**Power & Sample Size Justification**

We estimate that 52 evaluable patients (a total of 75 participants allowing for 30% of participants with missing or incomplete data) will have ≥80% power to detect at least 0.4 standard deviation (SD) change on the delayed recall measure of the HVLT-R post-RT. The power analysis is based on a paired t-test with a two-sided significance level of 0.05.

**Analysis Plan**

Graphical methods will be used to explore the cognitive test and imaging data, to visually describe and compare distributions of continuous variables, and to visualize results of statistical analyses. Quantitative imaging metrics (cortical thickness, subcortical volume, FA, MD, AD, RD, local efficiency, and clustering coefficient) will be analyzed to investigate their relationships with RT dose and cognitive measures. Comparisons between raw scores on cognitive tests and imaging metrics pre and post-RT will be performed using paired t-tests and Wilcoxon signed-rank tests. Pearson and Spearman correlation analyses will be used to assess associations between pairs of continuous measures. Multivariate mixed effect regression models will be used to evaluate the relationships of cognitive tests at 6-month and 12-month visits with RT dose to ROIs known to be instrumental in the specific cognitive domain adjusting for the baseline cognitive test, imaging parameters, age, gender, tumor laterality, and tumor type. During the analyses, false discovery rate (FDR) method will be used to account for multiple comparisons (103). All statistical analyses will be performed using R (R Foundation for Statistical Computing, Vienna, Austria) or SAS 9.4.

## DISCUSSION & CONCLUSION

RICD is an important target of efforts to use more sophisticated radiation techniques such as intensity modulated radiation therapy and proton therapy in order to decrease side effects (104). While validated dose constraints exist for structures such as the brainstem, cochlea, optic nerves and chiasm, and pituitary gland (28), development of dose constraints for intracranial structures involved in cognition is a new and exciting area of research that promises to improve radiation outcomes. Despite conformal dose reduction to the hippocampi, RICD occurs in a large percentage of patients, reflecting the

complexity of memory formation and the need to identify non-hippocampal structures involved in higher cognitive functions. The pathology underlying RICD likely begins prior to any gross anatomical changes or noticeable differences in cognition observed by the patient. Accordingly, development of quantitative in vivo biomarkers is essential for developing dose constraints and monitoring RICD.

This study utilizes conventional and advanced MRI, neurocognitive testing, and dosimetry information to provide a comprehensive description of RICD in patients with brain tumors receiving radiation therapy. The proposed analyses will provide insight into which intracranial structures are particularly susceptible to RT and how they modulate changes in cognition via aberrant network topology. The results of this study will help to provide dose constraints to better avoid cognitive decline that can ultimately be used to create radiation plans associated with less cognitive change. Incorporation of rs-fMRI into treatment planning and monitoring has the potential to improve cognitive outcomes in the setting of RT and provide personalized treatment. Additionally, utilization of graph theory will be able to identify specific nodes and hubs within brain networks that are susceptible to RT at the population and individual level (105).

This protocol and analysis pipeline will aid researchers interested in combining MRI imaging data including segmentation of intracranial structures not used in standard radiation planning with radiation dosimetry information to advance our understanding of RICD. We provide detailed information on study design, clinical and imaging protocols and analysis pipeline with which to investigate RT-induced cognitive changes on intracranial structures that are not segmented with standard radiation planning software. This is an important and complex process which should be transparent, and one of our goals with this paper is to promote utilization of open software packages in a useful and standardized way for the radiation oncology community.

## ETHICS AND DISSEMINATION

Studies involving human participants are reviewed and approved by the Research Subjects Review Board at the University of Rochester . All patients/participants provide their written informed consent to participate in this study. All results will be presented at relevant conferences and published in relevant peer-reviewed journals.

## AUTHOR CONTRIBUTIONS

Sara J Hardy: Protocol development and design, principal investigator, manuscript editing
Alan Finkelstein: Development of MRI pipeline for processing and analysis, manuscript editing
Eva Culakova: Development of statistical plan and power analysis, manuscript editing
Kenneth Usuki: Mentorship on clinical aspects of protocol and recruitment, manuscript editing
Jianhui Zhong: MRI protocol development, manuscript editing
Michelle Janelsins: Research mentorship in cognitive assessment and cohort studies, help with protocol development, manuscript editing
Giovanni Schifitto: Research mentorship in neuroimaging, help with protocol development and manuscript editing
Michael Milano: Research mentorship in evaluation of radiation toxicity, help with protocol development and manuscript editing
Nimish Mohile: Research mentorship in neuro-oncology, help with protocol development and manuscript editing
Madalina Tivarus: MRI protocol development, manuscript editing
Edward Lin: MRI protocol development, manuscript editing

Miriam Weber: Clinical neuropsychology, development of cognitive battery and interpretation of cognitive data, manuscript editing

## FUNDING

This work is supported by the Department of Radiation Oncology (internal funding), Wilmot Fellowship Award to Dr. Hardy, Schmitt Foundation Grant number GR505052 (PI: Hardy), DP2195765 and R01CA231014 (PI: Michelle Janelsins), R01MH118020 and R01AG054328 (PI: Schifitto), and the Cancer Control Clinical Research Training Program in the Dept. of Surgery. The project described in this publication was also supported by the University of Rochester CTSA award number UL1TR002001 from the National Center for Advancing Translational Sciences of the National Institutes of Health. The content is solely the responsibility of the authors and does not necessarily represent the official views of the National Institutes of Health.

## CONFLICT OF INTEREST STATEMENT

The authors declare that the research was conducted in the absence of any commercial or financial relationships that could be construed as a potential conflict of interest.

## ACKNOWLEDGEMENTS

Support from the Department of Radiation Oncology at University of Rochester

## REFERENCES

1. Taphoorn MJ, Klein M. Cognitive deficits in adult patients with brain tumours. Lancet Neurol. 2004;3(3):159-68.
2. Klaver KM, Duijts SFA, Engelhardt EG, Geusgens CAV, Aarts MJB, Ponds R, et al. Cancer-related cognitive problems at work: experiences of survivors and professionals. J Cancer Surviv. 2020;14(2):168-78.
3. Harrison RA, Wefel JS. Neurocognitive Function in Adult Cancer Patients. Neurol Clin. 2018;36(3):653-74.
4. Salans M, Tibbs MD, Huynh-Le MP, Yip A, Tringale K, Karunamuni R, et al. Quality of Life Is Independently Associated With Neurocognitive Function in Patients With Brain Tumors: Analysis of a Prospective Clinical Trial. Int J Radiat Oncol Biol Phys. 2021;111(3):754-63.
5. Pazzaglia S, Briganti G, Mancuso M, Saran A. Neurocognitive Decline Following Radiotherapy: Mechanisms and Therapeutic Implications. Cancers (Basel). 2020;12(1).
6. Hardy SJ, Krull KR, Wefel JS, Janelsins M. Cognitive Changes in Cancer Survivors. Am Soc Clin Oncol Educ Book. 2018;38:795-806.
7. Coomans MB, van der Linden SD, Gehring K, Taphoorn MJB. Treatment of cognitive deficits in brain tumour patients: current status and future directions. Curr Opin Oncol. 2019;31(6):540-7.
8. Makale MT, McDonald CR, Hattangadi-Gluth JA, Kesari S. Mechanisms of radiotherapy-associated cognitive disability in patients with brain tumours. Nat Rev Neurol. 2017;13(1):52-64.
9. Greene-Schloesser D, Moore E, Robbins ME. Molecular pathways: radiation-induced cognitive impairment. Clin Cancer Res. 2013;19(9):2294-300.
10. Greene-Schloesser D, Robbins ME. Radiation-induced cognitive impairment--from bench to bedside. Neuro Oncol. 2012;14 Suppl 4:iv37-44.

11. Michaelidesova A, Konirova J, Bartunek P, Zikova M. Effects of Radiation Therapy on Neural Stem Cells. Genes (Basel). 2019;10(9).
12. Bellinzona M, Gobbel GT, Shinohara C, Fike JR. Apoptosis is induced in the subependyma of young adult rats by ionizing irradiation. Neurosci Lett. 1996;208(3):163-6.
13. Lumniczky K, Szatmari T, Safrany G. Ionizing Radiation-Induced Immune and Inflammatory Reactions in the Brain. Front Immunol. 2017;8:517.
14. Constanzo J, Midavaine E, Fouquet J, Lepage M, Descoteaux M, Kirby K, et al. Brain irradiation leads to persistent neuroinflammation and long-term neurocognitive dysfunction in a region-specific manner. Prog Neuropsychopharmacol Biol Psychiatry. 2020;102:109954.
15. Wu PH, Coultrap S, Pinnix C, Davies KD, Tailor R, Ang KK, et al. Radiation induces acute alterations in neuronal function. PLoS One. 2012;7(5):e37677.
16. Weintraub NL, Jones WK, Manka D. Understanding radiation-induced vascular disease. J Am Coll Cardiol. 2010;55(12):1237-9.
17. Venkatesulu BP, Mahadevan LS, Aliru ML, Yang X, Bodd MH, Singh PK, et al. Radiation-Induced Endothelial Vascular Injury: A Review of Possible Mechanisms. JACC Basic Transl Sci. 2018;3(4):563-72.
18. Venkatesulu BP, Sanders KL, Hsieh CE, Kim BK, Krishnan S. Biomarkers of radiation-induced vascular injury. Cancer Rep (Hoboken). 2019;2(2):e1152.
19. Greene-Schloesser D, Robbins ME, Peiffer AM, Shaw EG, Wheeler KT, Chan MD. Radiation-induced brain injury: A review. Front Oncol. 2012;2:73.
20. Karunamuni R, Bartsch H, White NS, Moiseenko V, Carmona R, Marshall DC, et al. Dose-Dependent Cortical Thinning After Partial Brain Irradiation in High-Grade Glioma. Int J Radiat Oncol Biol Phys. 2016;94(2):297-304.
21. Seibert TM, Karunamuni R, Bartsch H, Kaifi S, Krishnan AP, Dalia Y, et al. Radiation Dose-Dependent Hippocampal Atrophy Detected With Longitudinal Volumetric Magnetic Resonance Imaging. Int J Radiat Oncol Biol Phys. 2017;97(2):263-9.
22. Huynh-Le MP, Karunamuni R, Moiseenko V, Farid N, McDonald CR, Hattangadi-Gluth JA, et al. Dose-dependent atrophy of the amygdala after radiotherapy. Radiother Oncol. 2019;136:44-9.
23. Kang J, Kim W, Seo H, Kim E, Son B, Lee S, et al. Radiation-induced overexpression of transthyretin inhibits retinol-mediated hippocampal neurogenesis. Sci Rep. 2018;8(1):8394.
24. Ji S, Ding X, Ji J, Wu H, Sun R, Li X, et al. Cranial irradiation inhibits hippocampal neurogenesis via DNMT1 and DNMT3A. Oncol Lett. 2018;15(3):2899-904.
25. Ben Abdallah NM, Slomianka L, Lipp HP. Reversible effect of X-irradiation on proliferation, neurogenesis, and cell death in the dentate gyrus of adult mice. Hippocampus. 2007;17(12):1230-40.
26. Mineyeva OA, Bezriadnov DV, Kedrov AV, Lazutkin AA, Anokhin KV, Enikolopov GN. Radiation Induces Distinct Changes in Defined Subpopulations of Neural Stem and Progenitor Cells in the Adult Hippocampus. Front Neurosci. 2018;12:1013.
27. Okoukoni C, McTyre ER, Ayala Peacock DN, Peiffer AM, Strowd R, Cramer C, et al. Hippocampal dose volume histogram predicts Hopkins Verbal Learning Test scores after brain irradiation. Adv Radiat Oncol. 2017;2(4):624-9.
28. Scoccianti S, Detti B, Gadda D, Greto D, Furfaro I, Meacci F, et al. Organs at risk in the brain and their dose-constraints in adults and in children: a radiation oncologist's guide for delineation in everyday practice. Radiother Oncol. 2015;114(2):230-8.
29. Kazda T, Jancalek R, Pospisil P, Sevela O, Prochazka T, Vrzal M, et al. Why and how to spare the hippocampus during brain radiotherapy: the developing role of hippocampal avoidance in cranial radiotherapy. Radiat Oncol. 2014;9:139.

30. Gondi V, Tolakanahalli R, Mehta MP, Tewatia D, Rowley H, Kuo JS, et al. Hippocampal-sparing whole-brain radiotherapy: a "how-to" technique using helical tomotherapy and linear accelerator-based intensity-modulated radiotherapy. Int J Radiat Oncol Biol Phys. 2010;78(4):1244-52.
31. Gondi V, Tome WA, Mehta MP. Why avoid the hippocampus? A comprehensive review. Radiother Oncol. 2010;97(3):370-6.
32. Gondi V, editor Preservation of Neurocognitive Function with Conformal Avoidance of the Hippocampus during Whole-Brain Radiotherapy for Brain Metastases: Preliminary Results of Phase III Trial NRG Oncology CC001. Annual Meeting of the American Society for Radiation Oncology; 2018; San Antonio, TX.
33. Huynh-Le MP, Tibbs MD, Karunamuni R, Salans M, Tringale KR, Yip A, et al. Microstructural Injury to Corpus Callosum and Intrahemispheric White Matter Tracts Correlate With Attention and Processing Speed Decline After Brain Radiation. Int J Radiat Oncol Biol Phys. 2021;110(2):337-47.
34. Tringale KR, Nguyen T, Bahrami N, Marshall DC, Leyden KM, Karunamuni R, et al. Identifying early diffusion imaging biomarkers of regional white matter injury as indicators of executive function decline following brain radiotherapy: A prospective clinical trial in primary brain tumor patients. Radiother Oncol. 2019;132:27-33.
35. Tibbs MD, Huynh-Le MP, Karunamuni R, Reyes A, Macari AC, Tringale KR, et al. Microstructural Injury to Left-Sided Perisylvian White Matter Predicts Language Decline After Brain Radiation Therapy. Int J Radiat Oncol Biol Phys. 2020;108(5):1218-28.
36. Tringale KR, Nguyen TT, Karunamuni R, Seibert T, Huynh-Le MP, Connor M, et al. Quantitative Imaging Biomarkers of Damage to Critical Memory Regions Are Associated With Post-Radiation Therapy Memory Performance in Brain Tumor Patients. Int J Radiat Oncol Biol Phys. 2019;105(4):773-83.
37. Sporns O, Tononi G, Kotter R. The human connectome: A structural description of the human brain. PLoS Comput Biol. 2005;1(4):e42.
38. Baliyan V, Das CJ, Sharma R, Gupta AK. Diffusion weighted imaging: Technique and applications. World J Radiol. 2016;8(9):785-98.
39. Tournier JD, Mori S, Leemans A. Diffusion tensor imaging and beyond. Magn Reson Med. 2011;65(6):1532-56.
40. Le Bihan D, Mangin JF, Poupon C, Clark CA, Pappata S, Molko N, et al. Diffusion tensor imaging: concepts and applications. J Magn Reson Imaging. 2001;13(4):534-46.
41. Wang S, Wu EX, Qiu D, Leung LH, Lau HF, Khong PL. Longitudinal diffusion tensor magnetic resonance imaging study of radiation-induced white matter damage in a rat model. Cancer Res. 2009;69(3):1190-8.
42. Milic M, Rees JH. Acute demyelination following radiotherapy for glioma: a cautionary tale. Pract Neurol. 2017;17(1):35-8.
43. Chapman CH, Zhu T, Nazem-Zadeh M, Tao Y, Buchtel HA, Tsien CI, et al. Diffusion tensor imaging predicts cognitive function change following partial brain radiotherapy for low-grade and benign tumors. Radiother Oncol. 2016;120(2):234-40.
44. Henderson F, Abdullah KG, Verma R, Brem S. Tractography and the connectome in neurosurgical treatment of gliomas: the premise, the progress, and the potential. Neurosurg Focus. 2020;48(2):E6.
45. Parker D, Ould Ismail AA, Wolf R, Brem S, Alexander S, Hodges W, et al. Freewater estimatoR using iNtErpolated iniTialization (FERNET): Characterizing peritumoral edema using clinically feasible diffusion MRI data. PLoS One. 2020;15(5):e0233645.

46. Chapman CH, Nagesh V, Sundgren PC, Buchtel H, Chenevert TL, Junck L, et al. Diffusion tensor imaging of normal-appearing white matter as biomarker for radiation-induced late delayed cognitive decline. Int J Radiat Oncol Biol Phys. 2012;82(5):2033-40.
47. Nagesh V, Tsien CI, Chenevert TL, Ross BD, Lawrence TS, Junick L, et al. Radiation-induced changes in normal-appearing white matter in patients with cerebral tumors: a diffusion tensor imaging study. Int J Radiat Oncol Biol Phys. 2008;70(4):1002-10.
48. Bullmore E, Sporns O. Complex brain networks: graph theoretical analysis of structural and functional systems. Nat Rev Neurosci. 2009;10(3):186-98.
49. Suprano I, Delon-Martin C, Kocevar G, Stamile C, Hannoun S, Achard S, et al. Topological Modification of Brain Networks Organization in Children With High Intelligence Quotient: A Resting-State fMRI Study. Front Hum Neurosci. 2019;13:241.
50. Varangis E, Habeck CG, Razlighi QR, Stern Y. The Effect of Aging on Resting State Connectivity of Predefined Networks in the Brain. Front Aging Neurosci. 2019;11:234.
51. Openneer TJC, Marsman JC, van der Meer D, Forde NJ, Akkermans SEA, Naaijen J, et al. A graph theory study of resting-state functional connectivity in children with Tourette syndrome. Cortex. 2020;126:63-72.
52. Khazaee A, Ebrahimzadeh A, Babajani-Feremi A. Identifying patients with Alzheimer's disease using resting-state fMRI and graph theory. Clin Neurophysiol. 2015;126(11):2132-41.
53. Sjoerds Z, Stufflebeam SM, Veltman DJ, Van den Brink W, Penninx BW, Douw L. Loss of brain graph network efficiency in alcohol dependence. Addict Biol. 2017;22(2):523-34.
54. Caparelli EC, Ross TJ, Gu H, Liang X, Stein EA, Yang Y. Graph theory reveals amygdala modules consistent with its anatomical subdivisions. Sci Rep. 2017;7(1):14392.
55. Meunier D, Lambiotte R, Fornito A, Ersche KD, Bullmore ET. Hierarchical modularity in human brain functional networks. Front Neuroinform. 2009;3:37.
56. Power JD, Schlaggar BL, Lessov-Schlaggar CN, Petersen SE. Evidence for hubs in human functional brain networks. Neuron. 2013;79(4):798-813.
57. Bahrami N, Seibert TM, Karunamuni R, Bartsch H, Krishnan A, Farid N, et al. Altered Network Topology in Patients with Primary Brain Tumors After Fractionated Radiotherapy. Brain Connect. 2017;7(5):299-308.
58. Derks J, Kulik S, Wesseling P, Numan T, Hillebrand A, van Dellen E, et al. Understanding cognitive functioning in glioma patients: The relevance of IDH-mutation status and functional connectivity. Brain Behav. 2019;9(4):e01204.
59. Wefel JS, Noll KR, Rao G, Cahill DP. Neurocognitive function varies by IDH1 genetic mutation status in patients with malignant glioma prior to surgical resection. Neuro Oncol. 2016;18(12):1656-63.
60. Mitchell TJ, Seitzman BA, Ballard N, Petersen SE, Shimony JS, Leuthardt EC. Human Brain Functional Network Organization Is Disrupted After Whole-Brain Radiation Therapy. Brain Connect. 2020;10(1):29-38.
61. Duffau H. Why brain radiation therapy should take account of the individual structural and functional connectivity: Toward an irradiation "a la carte". Crit Rev Oncol Hematol. 2020;154:103073.
62. Li M, Zhang Q, Yang K. Role of MRI-Based Functional Imaging in Improving the Therapeutic Index of Radiotherapy in Cancer Treatment. Front Oncol. 2021;11:645177.
63. Redmond KJ, Hildreth M, Sair HI, Terezakis S, McNutt T, Kleinberg L, et al. Association of Neuronal Injury in the Genu and Body of Corpus Callosum After Cranial Irradiation in Children With Impaired Cognitive Control: A Prospective Study. Int J Radiat Oncol Biol Phys. 2018;101(5):1234-42.

64. Redmond KJ, Milano MT, Kim MM, Trifiletti DM, Soltys SG, Hattangadi-Gluth JA. Reducing Radiation-Induced Cognitive Toxicity: Sparing the Hippocampus and Beyond. Int J Radiat Oncol Biol Phys. 2021;109(5):1131-6.
65. Milano MT, Grimm J, Niemierko A, Soltys SG, Moiseenko V, Redmond KJ, et al. Single- and Multifraction Stereotactic Radiosurgery Dose/Volume Tolerances of the Brain. Int J Radiat Oncol Biol Phys. 2021;110(1):68-86.
66. Wefel JS, Vardy J, Ahles T, Schagen SB. International Cognition and Cancer Task Force recommendations to harmonise studies of cognitive function in patients with cancer. Lancet Oncol. 2011;12(7):703-8.
67. Shapiro AM, Benedict RH, Schretlen D, Brandt J. Construct and concurrent validity of the Hopkins Verbal Learning Test-revised. Clin Neuropsychol. 1999;13(3):348-58.
68. Rasmusson DX, Bylsma FW, Brandt J. Stability of performance on the Hopkins Verbal Learning Test. Arch Clin Neuropsychol. 1995;10(1):21-6.
69. Benton AL HK, Sivan AB. Controlled Oral Word Association Multilingual Aphasia Examination professional manual. Lutz, FL1978.
70. Gaudino EA, Geisler MW, Squires NK. Construct validity in the Trail Making Test: what makes Part B harder? J Clin Exp Neuropsychol. 1995;17(4):529-35.
71. Goul WR, Brown M. Effects of age and intelligence on trail making test performance and validity. Percept Mot Skills. 1970;30(1):319-26.
72. Janelsins MC, Heckler CE, Peppone LJ, Ahles TA, Mohile SG, Mustian KM, et al. Longitudinal Trajectory and Characterization of Cancer-Related Cognitive Impairment in a Nationwide Cohort Study. J Clin Oncol. 2018;36(32):Jco2018786624.
73. Fray PJ, Robbins TW. CANTAB battery: proposed utility in neurotoxicology. Neurotoxicol Teratol. 1996;18(4):499-504.
74. Robbins TW, James M, Owen AM, Sahakian BJ, McInnes L, Rabbitt P. Cambridge Neuropsychological Test Automated Battery (CANTAB): a factor analytic study of a large sample of normal elderly volunteers. Dementia. 1994;5(5):266-81.
75. Thavarajah N, Bedard G, Zhang L, Cella D, Beaumont JL, Tsao M, et al. Psychometric validation of the functional assessment of cancer therapy--brain (FACT-Br) for assessing quality of life in patients with brain metastases. Support Care Cancer. 2014;22(4):1017-28.
76. Minton O, Stone P. A systematic review of the scales used for the measurement of cancer-related fatigue (CRF). Ann Oncol. 2009;20(1):17-25.
77. Hinz A, Mehnert A, Kocalevent RD, Brähler E, Forkmann T, Singer S, et al. Assessment of depression severity with the PHQ-9 in cancer patients and in the general population. BMC Psychiatry. 2016;16:22.
78. Spielberger CD, Gorsuch, R. L., Lushene, R., Vagg, P. R., & Jacobs, G. A. . Manual for the State-Trait Anxiety Inventory. Consulting Psychologists Press. 1983.
79. Baker Frank DM, Zabora, James, Polland Adrienne, Dudley William. A POMS short form for cancer patients: Psychometric and structural evaluation. Psycho-oncology. 2002;11.
80. Dyk KV, Crespi CM, Petersen L, Ganz PA. Identifying Cancer-Related Cognitive Impairment Using the FACT-Cog Perceived Cognitive Impairment. JNCI Cancer Spectrum. 2019;4(1).
81. Wang JY, Abdi H, Bakhadirov K, Diaz-Arrastia R, Devous MD, Sr. A comprehensive reliability assessment of quantitative diffusion tensor tractography. Neuroimage. 2012;60(2):1127-38.
82. Jenkinson M, Bannister P, Brady M, Smith S. Improved optimization for the robust and accurate linear registration and motion correction of brain images. Neuroimage. 2002;17(2):825-41.

83. Desikan RS, Segonne F, Fischl B, Quinn BT, Dickerson BC, Blacker D, et al. An automated labeling system for subdividing the human cerebral cortex on MRI scans into gyral based regions of interest. Neuroimage. 2006;31(3):968-80.
84. McMahon SJ. The linear quadratic model: usage, interpretation and challenges. Phys Med Biol. 2018;64(1):01TR.
85. van Leeuwen CM, Oei AL, Crezee J, Bel A, Franken NAP, Stalpers LJA, et al. The alfa and beta of tumours: a review of parameters of the linear-quadratic model, derived from clinical radiotherapy studies. Radiat Oncol. 2018;13(1):96.
86. Law MY, Liu B. Informatics in radiology: DICOM-RT and its utilization in radiation therapy. Radiographics. 2009;29(3):655-67.
87. Iglesias JE, Insausti R, Lerma-Usabiaga G, Bocchetta M, Van Leemput K, Greve DN, et al. A probabilistic atlas of the human thalamic nuclei combining ex vivo MRI and histology. Neuroimage. 2018;183:314-26.
88. Woolrich MW, Jbabdi S, Patenaude B, Chappell M, Makni S, Behrens T, et al. Bayesian analysis of neuroimaging data in FSL. Neuroimage. 2009;45(1 Suppl):S173-86.
89. Smith SM, Jenkinson M, Woolrich MW, Beckmann CF, Behrens TE, Johansen-Berg H, et al. Advances in functional and structural MR image analysis and implementation as FSL. Neuroimage. 2004;23 Suppl 1:S208-19.
90. Jenkinson M, Beckmann CF, Behrens TE, Woolrich MW, Smith SM. Fsl. Neuroimage. 2012;62(2):782-90.
91. Smith SM. Fast robust automated brain extraction. Hum Brain Mapp. 2002;17(3):143-55.
92. Andersson JLR, Sotiropoulos SN. An integrated approach to correction for off-resonance effects and subject movement in diffusion MR imaging. Neuroimage. 2016;125:1063-78.
93. Basser PJ, Mattiello J, LeBihan D. Estimation of the effective self-diffusion tensor from the NMR spin echo. J Magn Reson B. 1994;103(3):247-54.
94. Hua K, Zhang J, Wakana S, Jiang H, Li X, Reich DS, et al. Tract probability maps in stereotaxic spaces: analyses of white matter anatomy and tract-specific quantification. Neuroimage. 2008;39(1):336-47.
95. Woolrich MW, Ripley BD, Brady M, Smith SM. Temporal autocorrelation in univariate linear modeling of FMRI data. Neuroimage. 2001;14(6):1370-86.
96. Evans AC, Janke AL, Collins DL, Baillet S. Brain templates and atlases. Neuroimage. 2012;62(2):911-22.
97. Kim JW, Andersson JL, Seifert AC, Sun P, Song SK, Dula C, et al. Incorporating non-linear alignment and multi-compartmental modeling for improved human optic nerve diffusion imaging. Neuroimage. 2019;196:102-13.
98. Salimi-Khorshidi G, Douaud G, Beckmann CF, Glasser MF, Griffanti L, Smith SM. Automatic denoising of functional MRI data: combining independent component analysis and hierarchical fusion of classifiers. Neuroimage. 2014;90:449-68.
99. Griffanti L, Salimi-Khorshidi G, Beckmann CF, Auerbach EJ, Douaud G, Sexton CE, et al. ICA-based artefact removal and accelerated fMRI acquisition for improved resting state network imaging. Neuroimage. 2014;95:232-47.
100. Sporns O. The human connectome: a complex network. Ann N Y Acad Sci. 2011;1224:109-25.
101. Sporns O. Structure and function of complex brain networks. Dialogues Clin Neurosci. 2013;15(3):247-62.
102. Rubinov M, Sporns O. Complex network measures of brain connectivity: uses and interpretations. Neuroimage. 2010;52(3):1059-69.

103. Benjamini Y, Hochberg Y. Controlling the False Discovery Rate: A Practical and Powerful Approach to Multiple Testing. Journal of the Royal Statistical Society: Series B (Methodological). 1995;57(1):289-300.
104. Cho B. Intensity-modulated radiation therapy: a review with a physics perspective. Radiat Oncol J. 2018;36(1):1-10.
105. Farahani FV, Karwowski W, Lighthall NR. Application of Graph Theory for Identifying Connectivity Patterns in Human Brain Networks: A Systematic Review. Front Neurosci. 2019;13:585.

**Figure 1.** Study schema

**Figure 2.** MRI Data Processing Pipeline. FC: Functional Connectivity; FA: Fractional Anisotropy; MD: Mean Diffusivity; AD: Axial Diffusivity; RD: Radial Diffusivity; DTI: Diffusion Tensor Imaging; SC: Structural Connectivity; GTV: Gross Target Volume; CT: Computed Tomography; RT: Radiotherapy; dMRI: Diffusion MRI; rs-fMRI: resting state functional MRI; FEAT: FMRI Expert Analysis Tool; MELODIC: Multivariate Exploratory Linear Optimized Decomposition into Independent Components; FIX: FMRIB's ICA-based Xnoisefier.

**Figure 3.** Representative Images from participant with vestibular schwannoma. (A) RT dose map from RT structure set, mapped to CT image, and scaled. (B) T1w structural image co-registered with CT image and RT dose map via affine transformation (yellow circle shows acoustic schwannoma). (C) T1w image with gross target volume (GTV, yellow circle) used to mask tumor prior to processing. (D) Subcortical and cortical structures obtained from brain parcellation, with vestibular schwannoma excluded (yellow arrow).

**Figure 4.** Representative functional connectivity correlation matrices. Matrices are computed using the Pearson correlation coefficient between every time course for all pairs of nodes. Matrices are thresholded at 0.5 and normalized. The average of all patient specific correlation matrices at baseline (A) and 6-months post RT (B). The color bar represents the normalized correlation coefficient between pairs of nodes.

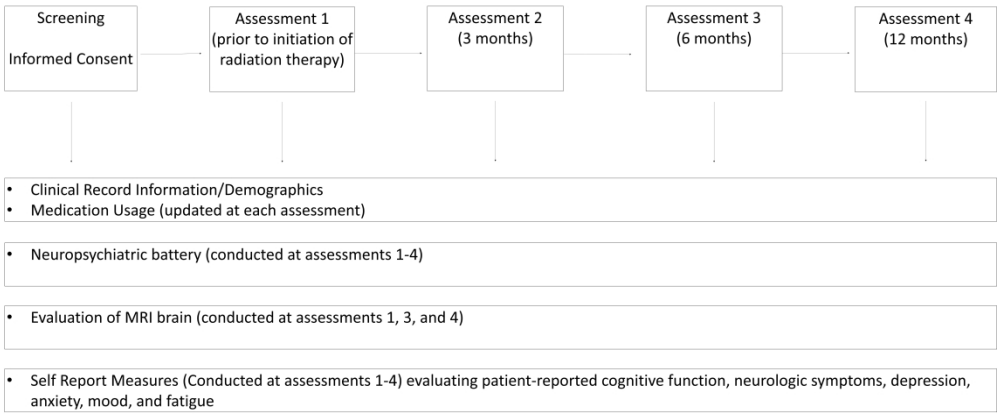


Study schema

1387x581mm (150 x 150 DPI)

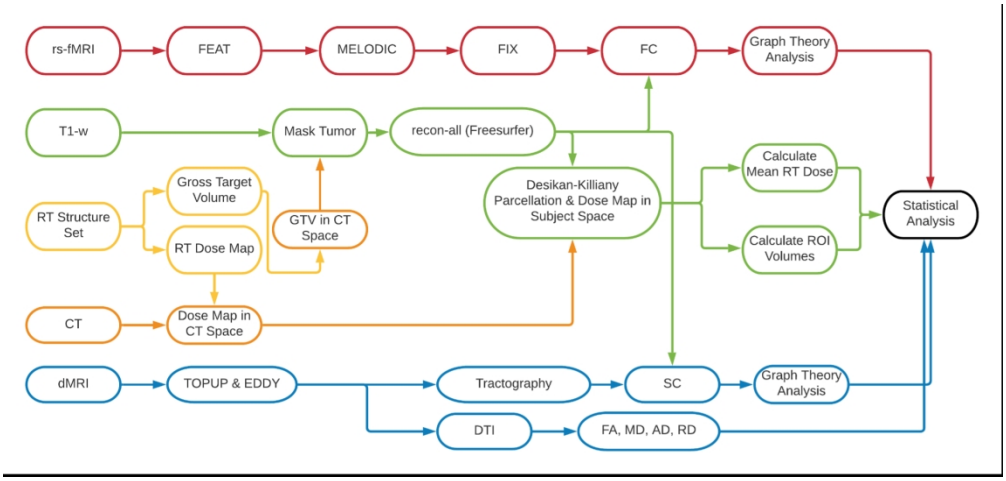


MRI Data Processing Pipeline. FC: Functional Connectivity; FA: Fractional Anisotropy; MD: Mean Diffusivity; AD: Axial Diffusivity; RD: Radial Diffusivity; DTI: Diffusion Tensor Imaging; SC: Structural Connectivity; GTV: Gross Target Volume; CT: Computed Tomography; RT: Radiotherapy; dMRI: Diffusion MRI; rs-fMRI: resting state functional MRI; FEAT: FMRI Expert Analysis Tool; MELODIC: Multivariate Exploratory Linear Optimized Decomposition into Independent Components; FIX: FMRIB's ICA-based Xnoisefier.

103x49mm (500 x 500 DPI)

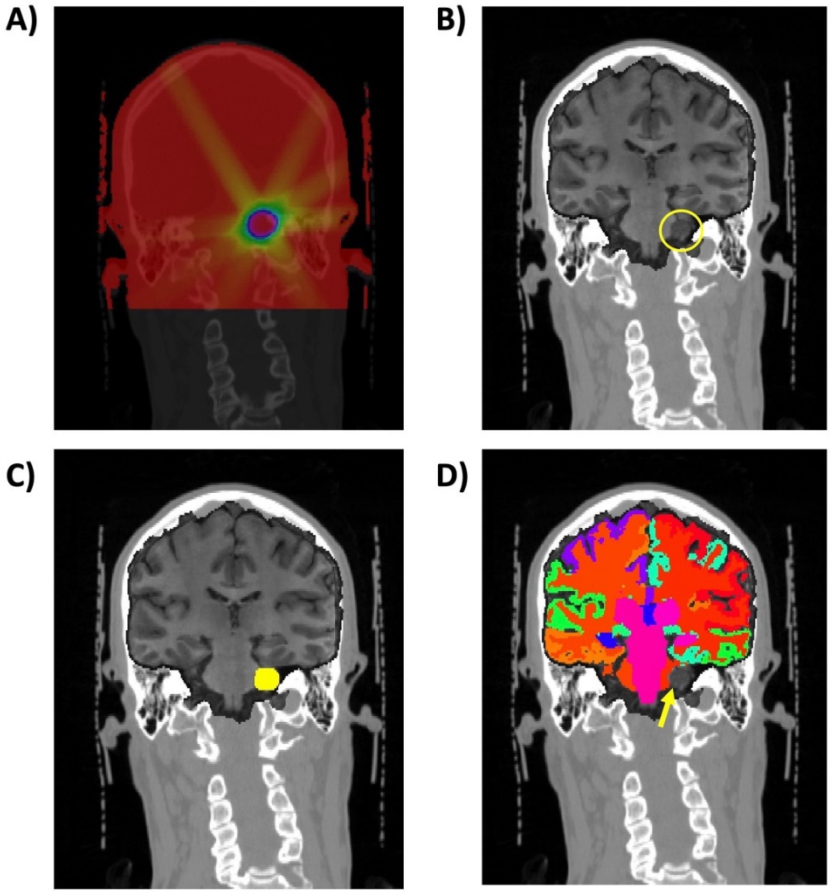


Representative Images from subject with vestibular schwannoma. (A) RT dose map from RT structure set, mapped to CT image, and scaled. (B) T1w structural image co-registered with CT image and RT dose map via affine transformation (yellow circle shows acoustic schwannoma). (C) T1w image with gross target volume (GTV, yellow circle) used to mask tumor prior to processing. (D) Subcortical and cortical structures obtained from brain parcellation, with vestibular schwannoma excluded (yellow arrow).

67x64mm (500 x 500 DPI)

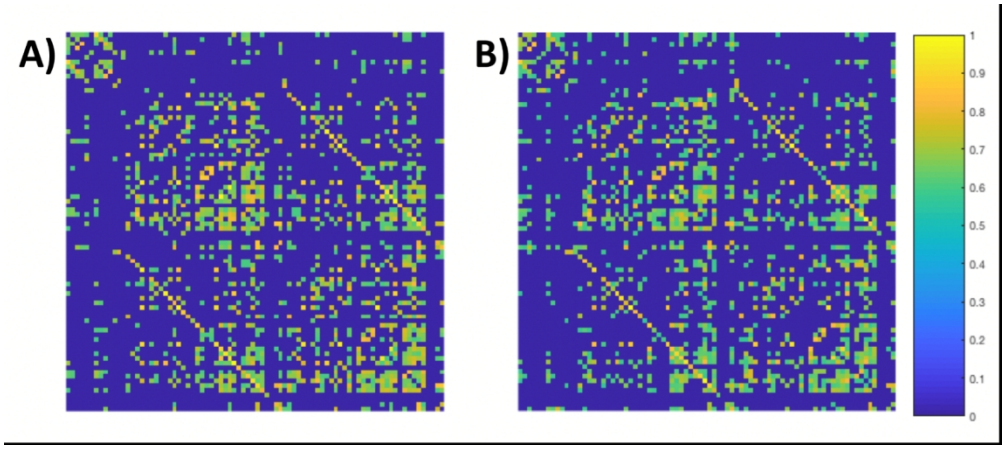


Representative functional connectivity correlation matrices. Matrices are computed using the Pearson correlation coefficient between every time course for all pairs of nodes. Matrices are thresholded at 0.5 and normalized. The average of all subject specific correlation matrices at baseline (A) and 6-months post RT (B). The color bar represents the normalized correlation coefficient between pairs of nodes.

88x38mm (500 x 500 DPI)